MC-ICP-MS 锂同位素溶液分析技术与应用

田世洪[1,2],路娜[1],侯增谦[3],苏本勋[4,5],肖燕[6],杨丹[2]

1)东华理工大学,核资源与环境国家重点实验室,南昌,330013;
2)中国地质科学院矿产资源研究所,自然资源部成矿作用与资源评价重点实验室,北京,100037;
3)中国地质科学院地质研究所,北京,100037;
4)中国科学院地质与地球物理研究所,矿产资源研究院重点实验室,北京,100029;
5)中国科学院大学,北京,100049;
6)中国科学院地质与地球物理研究所,岩石圈演化国家重点实验室,北京,100029

www.geojournals.cn/georev

内容提要:Li同位素是一种新兴的非传统稳定同位素示踪工具,在地质学、地球化学研究中具有广阔的应用前景。目前,Li同位素溶液分析技术主要采用热电离质谱仪(TIMS)和多接收电感耦合等离子质谱仪(MC-ICP-MS),与TIMS相比,MC-ICP-MS具有分析精度高、样品量少、测试速度快等诸多优点。本研究团队近年来建立了MC-ICP-MS高精度Li同位素分析方法,在天然样品、标准物质以及石英包裹体的Li同位素测定中都取得了良好结果。以此为依托,研究团队建立了适用于西藏本地岩石成因研究的Li同位素地质端元,并将Li同位素应用于青藏高原岩石圈结构及其隆升历史、川西碳酸岩型稀土矿床富集机制、四川呷村VMS型矿床成矿流体来源和四川甲基卡硬岩型Li矿床富集机理等方面。本文比较详细地综述了这些研究进展,旨在加深对Li同位素溶液分析技术的理解,展示其在地球化学研究中的良好应用前景。

关键词:Li同位素;MC-ICP-MS;地质端元;地质应用

锂(Li)是自然界最轻的金属元素,原子序数为3。Li有^{7}Li和^{6}Li两种稳定同位素,其天然丰度分别为92.48%和7.52%(Chan,1988),是自然界同一金属相对质量差最大的同位素,导致了Li同位素具有非常强的分馏作用,$\delta^{7}Li$值差异可高达80‰(图1;Tomascak et al., 2016; Penniston-Dorland et al., 2017;Liu Jiayi et al., 2020;赵悦等,2020)。在部分熔融、分离结晶、地表风化等作用过程中,^{6}Li偏向于保留在固相中,而^{7}Li易于进入熔/流体中(Rudnick et al., 2004;Kisakürek et al., 2005;Wunder et al., 2006;Xiao Yan et al., 2017)。Li是一种碱金属元素,由于Li^{+}和Mg^{2+}的离子半径比较接近(分别为0.059 nm和0.057 nm),在晶格中Li^{+}可以替代Mg^{2+},与镁(Mg)发生类质同象替代,Li可以置换橄榄石和辉石中的Mg,使Li在地幔部分熔融过程中显示出中等不相容的地球化学特征(Seitz and Woodland,2000)。对于多数地幔矿物而言,其分配系数介于0.1~1.0之间,因而能够在地幔和地壳中分布广泛(Ottolini et al., 2009)。Li同位素对交代富集作用非常敏感(Magna et al., 2008; Marschall et al., 2009; Halama et al., 2011; Xiao Yan et al., 2015)。以上这些特性使Li同位素体系广泛应用于示踪陆壳风化(Murphy et al., 2019; Li Wenshuai et al., 2020)、陨石和宇宙化学(Goderis et al., 2016; Tomascak et al., 2016; Pati et al., 2018)、板块俯冲及壳幔物质循环(Tian Shihong et al., 2015, 2020a; Hanna et al., 2020; Tan Dongbo et al., 2020; Tian Hengci et al., 2020)、卤水来源与演化(He Maoyong et al., 2020)、洋壳热液活动及蚀变(Liu Haiyang et al., 2019; Seyedali et al., 2021)、热液成矿作用(Nadeau et al., 2020)、稀有金属成矿过程(刘丽君等,2017; Chen Bin et al., 2018, 2020; 侯江龙等,

注:本文为国家自然科学基金资助项目(编号:41773014)、江西省"双千计划"创新领军人才长期项目和东华理工大学高层次人才引进配套经费资助项目(编号:1410000874)的成果。
收稿日期:2021-04-03;改回日期:2021-06-04;网络首发:2021-06-20;责任编辑:刘志强。Doi: 10.16509/j.georeview.2021.06.081
作者简介:田世洪,男,1973年生,研究员,博士研究生导师,主要从事同位素地球化学和矿床学研究工作;Email:s.h.tian@163.com。



图 1 地球主要储库的 Li 同位素组成(修改自 Tomascak et al., 2016;Penniston-Dorland et al., 2017;Liu Jiayi et al., 2020;赵悦等,2020)

Fig. 1 Li isotopic compositions of various reservoirs (modified from Tomascak et al., 2016; Penniston-Dorland et al., 2017; Liu Jiayi et al., 2020; Zhao Yue et al., 2020&)

2018; Li Jie et al., 2018)、地表水及地下水地球化学(Qi Huihui et al., 2019; Maffre et al., 2020)等重要的地质过程。

Li 同位素组成表示方法采用 δ^7Li 形式:

$$\delta^7\mathrm{Li}_{样品}=\frac{\left(^7\mathrm{Li}/^6\mathrm{Li}\right)_{样品}}{\left(^7\mathrm{Li}/^6\mathrm{Li}\right)_{标准}}-1\times1000‰$$

国际上通用的 Li 同位素标准参考物质有两种:一种是欧洲共同体联合研究中心核测量中心局(CBNM)的 IRMM-016(纯碳酸锂)(Michils and Bivre,1983),另一种是美国国家标准局(NIST)的 L-SVEC(纯碳酸锂; Flesch et al., 1973)。Li 同位素组成的测定方法主要有(苏嫒娜等,2011;李献华等,2015):原子吸收光谱(AAS)、热电离质谱(TIMS)、四级质谱(ICP-MS)、多接收器电感耦合等离子体质谱(MC-ICP-MS)、离子探针(Ion probe)、二次离子质谱仪(SIMS)以及激光多接收器电感耦合等离子体质谱(LA-MC-ICP MS)。离子探针、二次离子质谱仪和激光多接收器电感耦合等离子体质谱主要用于橄榄石、辉石等的原位 Li 同位素组成测量,缺点是分析精度较差(绝对误差约 1.0‰~3.4‰),优点是样品无需通过复杂的化学分离纯化过程(Zhang Hongfu et al., 2010; Su Benxun et al., 2012; 李献华等,2015)。Su Benxun 等(2015)通过大量测试和筛选,成功研发了 11 个原位分析的橄榄石、斜方辉石和单斜辉石 Li 同位素标样。热电离质谱是将样品中的 Li 通过化学分离方法提纯出来,转化成 $Li_2B_4O_7$ 或 Li_3PO_4 后测量 Li 同位素组成,分析精度可达 0.3‰,但存在以下不足(苏嫒娜等,2011):① 电离过程的分馏效应常导致分析结果失真;② 对样品的纯度要求苛刻,所需样品量多(约 250 ng Li);③ 分析时间较长,工作效率较低。

Tomascak 等(1999a,b)首次使用多接收器电感耦合等离子体质谱(MC-ICP-MS)分析 Li 同位素。该分析具有用量低、分析精度高、化学流程短和仪器分析省时等特点。为此,研究团队在自然资源部成矿作用与资源评价重点实验室建立了 MC-ICP-MS 高精度测试 Li 同位素方法(苏嫒娜等,2011; Tian Shihong et al., 2012),并加以地质应用示范研究。本文就西藏主要地质端元的 Li 同位素组成以及 Li 同位素在青藏高原岩石圈结构及其隆升历史、碳酸岩型稀土矿床富集机制、VMS 型矿床成矿流体来源和硬岩型 Li 矿床富集机理等方面的应用进行了总结,以期对拓展 Li 同位素的应用潜力提供启示。

1 MC-ICP-MS 锂同位素分析技术

1.1 天然样品的 Li 同位素测定

1.1.1 仪器、试剂和标样

锂、钙、钾、钠、铁和镁含量分析在清华大学分析中心原子吸收光谱仪(ICP-AES)上完成,精度为 0.01×10^{-6};Li 同位素组成分析在中国地质科学院矿产资源研究所 Neptune 型高分辨多接收器电感耦合等离子体质谱仪(MC-ICP-MS)上完成。该 MC-ICP-MS 由 Thermo Finnigan 公司制造,配置 5 个离子计数器(Ion Counting)和 9 个法拉第杯(包括 1 个中心杯和 8 个配置在中心杯两侧的法拉第杯),并以马达驱动进行精确的位置调节;最低质量数杯外侧装有 4 个离子计数器,中心杯后装有 1 个电子倍增器。采用动态变焦(ZOOM)专利技术,可将质量色散扩大至 17%,是一种双聚焦型(质量聚焦和能量聚焦)质谱仪(侯可军等,2008)。样品雾化后进入 Thermo Finnigan 公司生产的由气旋和斯克特雾化器相结合

的稳定进样系统(stable introduction system, SIS),可以缩短清洗时间并提供更为稳定的信号(侯可军等,2008)。而低含量样品则使用膜去溶(DSN)进样,可提高灵敏度并有效降低氮化物、氢氧化物和氧化物的干扰。

主要的化学试剂有 HNO_3、HCl、HF 以及无水乙醇,除无水乙醇(浓度为 99.9%)外,其余均由优级纯酸经过 Savillex DST-1000 亚沸蒸馏系统二次蒸馏所得。超纯水由 Millipure 纯化制得,电阻为 18.2 MΩ·cm。分离实验中用 3 组离子交换柱,每组为 12 根,前两组为聚丙烯柱,第三组为石英柱,每组分别填充 1.2 mL、1.5 mL 和 1.0 mL 阳离子交换树脂(AG 50W-X8,200~400 目)。

分析测试过程中用 4 种标样:AGV-2、BHVO-2、L-SVEC 和 IRMM-016,其中 BHVO-2 和 AGV-2 为标准岩石样品,L-SVEC 和 IRMM-016 用于 Li 同位素比值的计算。

1.1.2　实验流程

Li 同位素分析的具体实验流程包括:样品溶解、化学分离和质谱测试 3 个部分:

(1)样品溶解:一方面因为岩石样品与 HF 反应,生成结构不同的氟化物(Croudace,1980),Li 会赋存在这些氟化物中,即使加入 $HClO_4$ 也很难溶解(Ryan and Langmuir et al., 1987),另一方面由于 $HClO_4$ 需要在高温下(200 ℃)、数次添加 HNO_3 才能将其驱逐干净,且耗时较长,因此样品溶解过程中未加入 $HClO_4$。具体步骤为:① 将一定量样品(具体视样品中 Li 的含量而定)按照 HNO_3 : HF = 1 : 5 比例溶解于 Savillex PFA 敞口溶样瓶中。溶样时酸的用量与样品的质量成正比,本实验室一般为每 50 mg 样品用 0.8 mL HNO_3;② 拧紧溶样瓶,放在超声波中震荡 10 min,再置于加热板反应 24 h(温度为 100~120 ℃);③ 蒸干溶液后,加入 2~4 次一定量的浓 HNO_3(2.5 mL 或 50 mg 样品),每次均需蒸干;④ 将 1 mL 浓 HCl 加入样品中,在 100~120℃ 温度下加热,直到溶液完全变透明;⑤ 再次蒸干样品,将 1 mL 4 mol/L HCl 加入,作为备用。

(2)化学分离:天然样品的分离提纯,主要在参考 Rudnick 等(2004)和 Moriguti 等(1998)的化学分离实验步骤基础上,做了一定的改动(表 1)。主要程序为:① 交换柱 1 为 1.2 mL 阳离子交换树脂(AG50W-X8)填充的聚丙烯交换柱,粗略分离 K、Na、Ca、Fe、Mg 等主量元素,为保证 Li 回收率,将柱子 1 的接受区间划定为 1~6 mL,Li 的回收率为 101.2%~98.9%,平均值为 100.0%;② 交换柱 2 为 1.5 mL 阳离子交换树脂(AG50W-X8)填充的聚丙烯交换柱,分离除 Na 之外的主量元素,柱子 2 的接受范围划定为 1~23 mL,Li 的回收率为 101.9%~97.6%,平均值为 99.9%;③ 交换柱 3 为 1 mL 阳离子交换树脂(AG 50W-X8)填充的石英交换柱,将 Li 和 Na 分离,接受范围划定为 1~9 mL,一般需要二次过滤,Li 的回收率为 99.8%~103.3%,平均值为 100.6%。

(3)质谱测试:纯化后的 Li 溶液质量浓度约为 200 μg/L,以 2% HNO_3 溶液作为介质,通过喷雾器引入 Ar 等离子区。所有样品均使用 Thermo Finnigan Neptune 型 MC-ICP-MS 仪器测试,^7Li 和 ^6Li 使用两个相反的法拉第杯同时测量,前者位于高质量法拉第杯(H4),而后者位于低质量法拉第杯(L4)。仪器工作参数:RF 功率 1200 W,冷却气约 15 L/min,辅助气约 0.6 L/min,载气约 1.15 L/min,雾化器类型为 Menhard 雾化器(50 μL/min),分析

表 1 不同研究者使用的不同淋洗介质和树脂量

Table 1 Different eluants and resin heights used by differernt researchers

	柱子 1	柱子 2	柱子 3	参考文献
淋洗介质	2.8 mol/L HCl	0.15 mol/L HCl	0.5 mol/L HCl,30%乙醇	苏嫒娜等,2011
	0.15 mol/L HCl			汪齐连等,2006
	2.5 mol/L HCl	0.15 mol/L HCl	0.5 mol/L HCl,30%乙醇	Rudnick et al., 2004
	1 mol/L HNO_3,80%甲醇			Teng Fangzhen et al., 2004
	1 mol/L HNO_3,80%甲醇			Tomascak et al., 1999b
	2.8 mol/L HCl	0.15 mol/L HCl	0.5 mol/L HCl,30%乙醇	Moriguti and Nakamura,1998
树脂量	1.2 mL	1.5 mL	1.0 mL	苏嫒娜等,2011
	石英柱:内径 8 mm,树脂高度 300 mm			汪齐连等,2006
	1.0 mL	1.0 mL	1.0 mL	Rudnick et al., 2004
	12 mL 阳离子交换柱			Teng Fangzhen et al., 2004
	石英柱:内径 8 mm,树脂高度 300 mm			Tomascak et al., 1999b
	1.0 mL	1.0 mL	1.0 mL	Moriguti and Nakamura,1998

器真空 4~8 nPa。研究结果表明,当 Na/Li≤20 时,纯碳酸锂的 δ^7Li 值并未产生较大变化,仍然在误差范围内(苏嫒娜等, 2011; Tian Shihong et al., 2012)。因此,工作测试开始时,先对 Na/Li 进行半矢量化测试,若 Na/Li>20 则需对样品重新过第三根柱子,进一步分离 Na。对于 Li 同位素,通过使用标准—样品交叉法(Standard—Sample—Bracketing, SSB),可以对其进行校正:空白 1 ⟶标样 1 ⟶空白 2 ⟶样品 1 ⟶空白 3 ⟶标样 2 ⟶空白 4 ⟶样品 2。测试结果表示为:$\delta^7Li=[(R_{SP}/R_{ST})-1]\times1000‰$,其中 R_{SP} 为样品$^7Li/^6Li$ 值的测定值,R_{ST} 为与样品相邻的两次标样$^7Li/^6Li$ 值测定值的平均。所用同位素标准为 L-SVEC 或者 IRMM-016,许多学者用 NIST L-SVEC 对 IRMM-016 的测试值约为 -0.1‰,远远小于测试误差±1‰,因此 IRMM-016 与 L-SVEC 可以相互替代。测样时每组收集 20 个数据,共采集 2~4 组数据,$^7Li/^6Li$ 测量精度≤ ±0.2‰(2σ)。每两次测试之间,用 2% 和 5%的 HNO_3 清洗系统约 10 min。测试中 Li 质量浓度为 200 μg/L 时,^{7}Li 的信号为 20 V 左右,^{6}Li 的信号值约 1.5 V。

1.1.3 分析结果

国际标样 AGV-2(相对于 IRMM-016)、IRMM-016(相对于 L-SVEC)和 BHVO-2(相对于 IRMM-016)的 δ^7Li 值分别为(5.68±1.04)‰(2σ, n=18)、(-0.01±0.72)‰(2σ, n=15)和(4.33±0.76)‰(2σ, n=18;图 2;苏嫒娜等, 2011; Tian Shihong et al., 2012),与前人分析结果相吻合,分析精度与国际同类实验室水平相当(Bouman et al., 2004; Rudnick et al., 2004; Jeffcoate et al., 2004; Magna et al., 2004; Marschall et al., 2007; Rosner et al., 2007; Qiu et al., 2009)。

1.2 标准物质的 Li 同位素测定

稳定同位素测试需要通过与标准物质的对比,确定样品的同位素组成,通过地质标准物质监控化学分析和质谱测试流程,评估分析不确定度和稳定性,以便各个实验室间进行数据比较。目前国际上通用的 Li 同位素标准参考物质是欧盟参考物质及测量研究所(IRMM)研制的纯碳酸锂 IRMM-016 和美国国家标准技术研究院(NIST)研制的纯碳酸锂 L-SVEC,两者的 Li 同位素组成基本一致(苏嫒娜等,2011; Tian Shihong et al., 2012)。为此,赵悦等(2015)选用纯碳酸锂标样 IRMM-016、L-SVEC,安山岩标样 AGV-2,玄武岩标样 BHVO-2、JB-2 和 BCR-2 以及霞石岩标样 NKT-1,参照苏嫒娜等(2011)和 Tian Shihong 等(2012)的描述,对这 7 种常用地质标准物质采用硝酸—氢氟酸混合酸进行消解,通过 3 根阳离子交换树脂(AG50W-X8,200~400 目)填充的聚丙烯交换柱和石英交换柱对 Li 进行分离富集,利用 Neptune 型多接收器电感耦合等离子体质谱(MC-ICP-MS)测定这些标准物质的 Li 同位素比值,使用标准—样品交叉法校正仪器的质量分馏,样品进样溶液和标准样品的浓度相对偏差控制在 10%以内,测定样品之前,先测定国际 Li 标准物质 IRMM-016 配制的标准溶液或者实验室标准溶液 CAGS-Li 的同位素丰度比值,待$^7Li/^6Li$ 值稳定,IRMM-016 的同位素比值在误差范围内与真值一致或者实验室标样

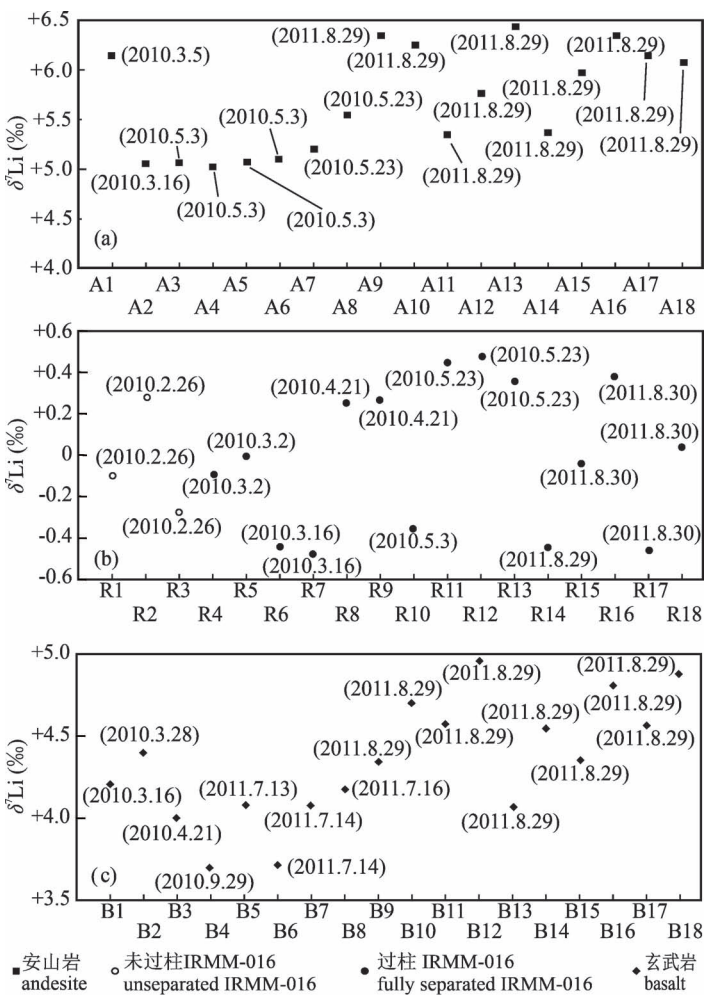


图 2 安山岩、IRMM-016、玄武岩的 Li 同位素分析结果
(据 Tian Shihong et al., 2012)

Fig. 2 Analytical results of andesite, IRMM-016 and basalt
(from Tian Shihong et al., 2012)

测定数据稳定在长期监测范围内,方可进行样品测试。此外,在基质效应的研究中,使用不同量的 IRMM-016 配制的标准溶液过柱,结果表明,在现有测试精度下,只要分析样品的 Li 含量达到 100 μg/L,且不超过树脂的承载量,样品的 Li 同位素组成在误差范围内与真值吻合,样品量的大小不影响 Li 同位素测定结果的准确性。

上述 7 种常用地质标准物质的 Li 同位素组成与测试精度分别为(图 3,图 4):

$\delta^7Li_{BHVO\text{-}2—L\text{-}SVEC}=4.7‰\pm1.0‰(2\sigma,n=53)$,

$\delta^7Li_{JB\text{-}2—L\text{-}SVEC}=4.9‰\pm1.0‰(2\sigma,n=20)$,

$\delta^7Li_{BCR\text{-}2—L\text{-}SVEC}=4.4‰\pm0.8‰(2\sigma,n=8)$,

$\delta^7Li_{AGV\text{-}2—L\text{-}SVEC}=6.1‰\pm0.4‰(2\sigma,n=14)$,

$\delta^7Li_{NKT\text{-}1—L\text{-}SVEC}=9.8‰\pm0.2‰(2\sigma,n=3)$,

$\delta^7Li_{L\text{-}SVEC—L\text{-}SVEC}=0.2‰\pm0.3‰(2\sigma,n=16$,未过柱),

$\delta^7Li_{L\text{-}SVEC—L\text{-}SVEC}=-0.3‰\pm0.3‰(2\sigma,n=10$,过柱),

$\delta^7Li_{IRMM\text{-}016—L\text{-}SVEC}=-0.1‰\pm0.3‰(2\sigma,n=20$,未过柱),

$\delta^7Li_{IRMM\text{-}016—L\text{-}SVEC}=0.0‰\pm0.5‰(2\sigma,n=10$,过柱),

这些数据在误差范围内与国际上已发表的数据一致(Bouman et al., 2004; Rudnick et al., 2004; Jeffcoate et al., 2004; Magna et al., 2004; Marschall et al., 2007; Rosner et al., 2007; Qiu et al., 2009; 苏媛娜等,2011),表明该实验室建立的 Li 同位素方法是可靠的。Li 同位素分析精度可以达到大约 0.5‰,长期的分析精度即外部重现性≤±1.0‰,达到国际同类实验室水平。这些常用地质标准物质的 Li 同位素组成数据的发表为 Li 同位素研究提供了统一的标准,使地质样品的 Li 同位素数据的质量监控成为可能。

1.3　石英包裹体的 Li 同位素测定

由于 Li 在流体中的氯化物络合行为(Candela and Piccoli, 1995)、强的流体活动性(You et al., 1996)和大的同位素分馏(Tomascak et al., 2016; Penniston-Dorland et al., 2017),Li 同位素已被证明是流体相关过程的重要地球化学示踪剂。Li 同位素分馏可以用来示踪热液体系中矿物的沉淀和/或扩散。对热液矿床来说,石英是最常见的脉石矿物,以包裹体形式捕获成矿流体,它的 Li 同位素体系具有限制流体来源和定量不同来源的流体流量的潜力。为此,Yang Dan 等(2015)率先研发了石英包

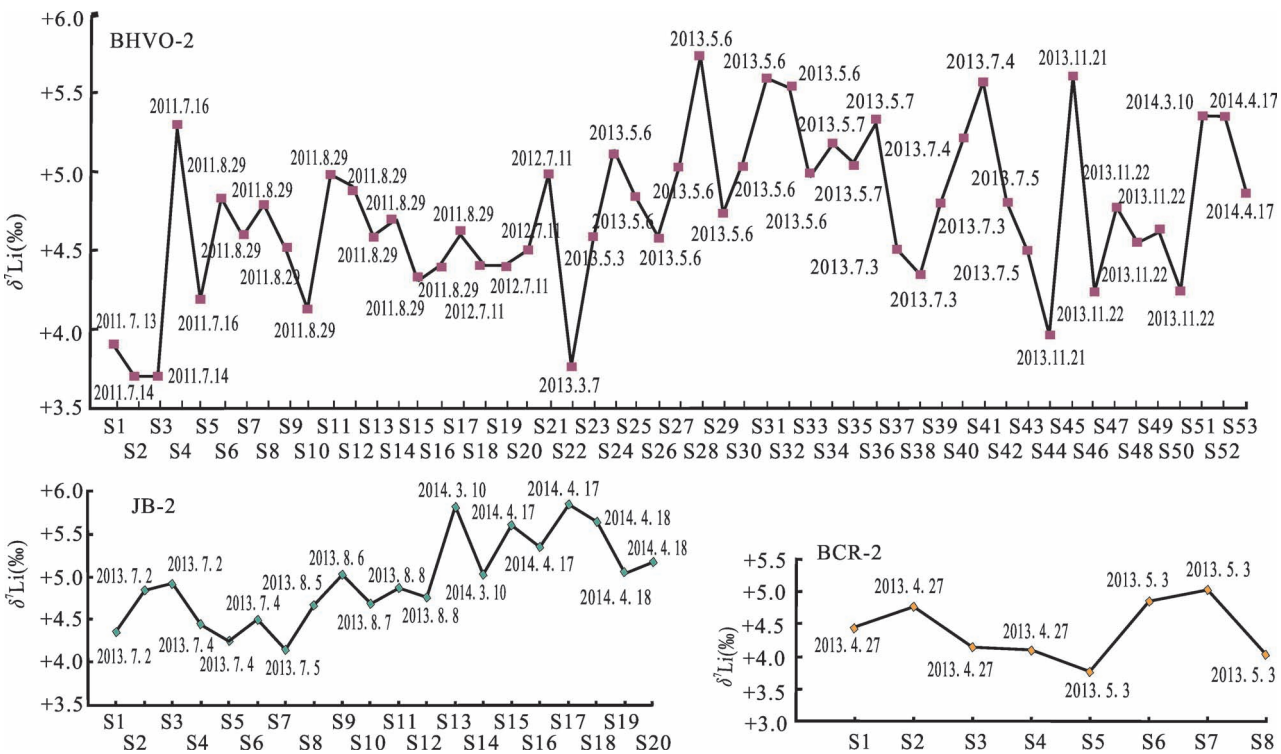


图 3 国际标准物质 BHVO-2、JB-2、BCR-2 的 Li 同位素组成长期测定结果(据赵悦等,2015)

Fig. 3 Analytical results of Li isotopic ratios of BHVO-2, JB-2, BCR-2 in the long-term measurement (from Zhao Yue et al., 2015&)

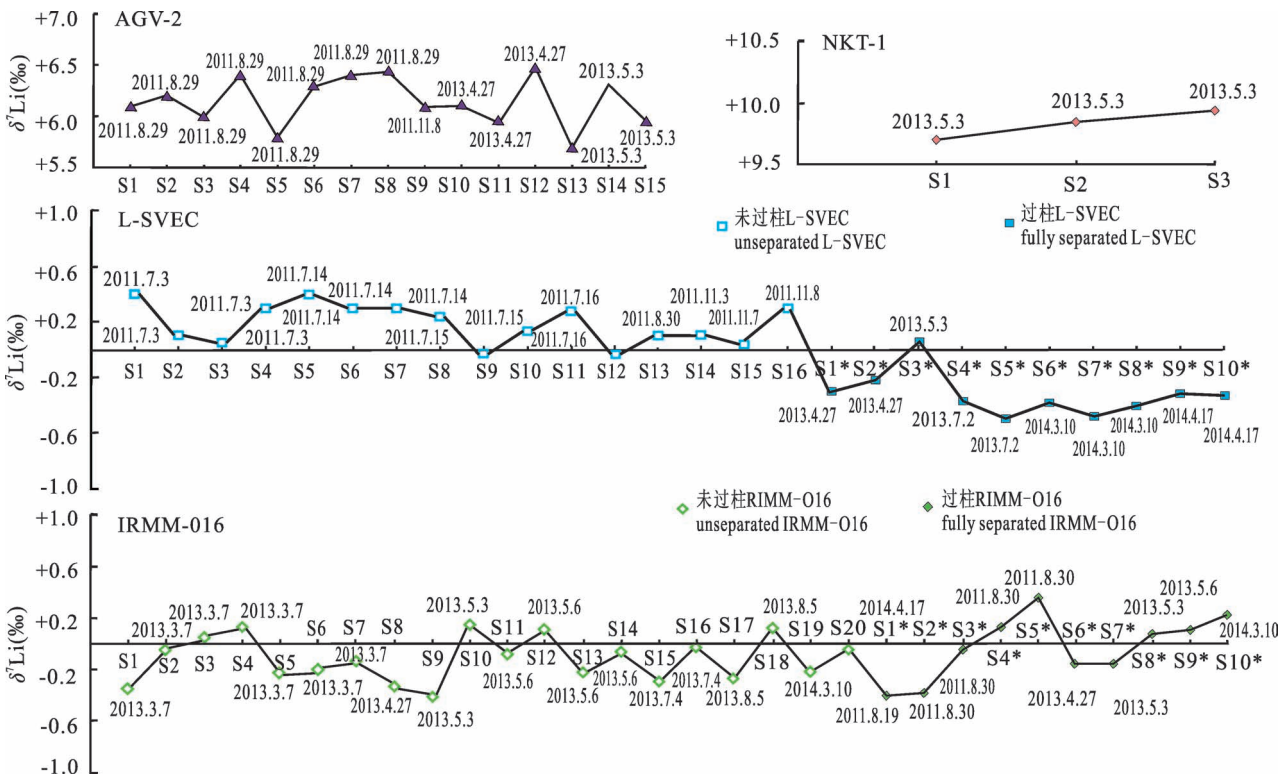


图 4 国际标准物质 AGV-2、NKT-1、L-SVEC、IRMM-016 的 Li 同位素组成长期测定结果(据赵悦等,2015)

Fig. 4 Analytical results of Li isotopic ratios of AGV-2, NKT-1, L-SVEC, IRMM-016 in the long-term measurement (from Zhao Yue et al., 2015&)

裹体 Li 同位素处理方法,实验流程包括如下几个方面:

(1)样品表面净化:在采集石英样品的时候尽量选择无穿插关系的石英大脉体,在挑选石英单矿物之前进行显微岩相学观察,确定无后期石英脉。将挑选好的纯度大于 99%的石英单矿物样品加入适量王水(HCl—HNO_3 按 3∶1 混合)放置于加热板 120℃恒温 3 h,这样可将次生包裹体爆裂去除。倾去残余酸并用超纯水清洗,洗至洗涤液电导与超纯水电导一致,可保证爆裂开的次生流体包裹体成分和石英表面杂质都清除干净。再用纯水浸泡过夜。倾去浸泡液,加入超纯水,用超声波清洗器清洗样品数分钟,立即抽滤,并用超纯水洗涤数次,样品置于瓷皿中,于 100 ℃烘干。

(2)样品量:海底喷流—沉积形成的火山成因块状硫化物矿床石英样品 4 g 左右,斑岩型矿床石英脉样品>0.5 g,1 g 左右最好,无论是提取流体包裹体液相还是石英本身,Li 含量都可以满足测试需要。

(3)研磨法打开流体包裹体:将称量好的样品磨制到 350 目以上后(经咨询,样品磨制单位没有更高目数的样品筛),仍继续磨制一段时间,争取达到 500 目以上,此时可以认为流体包裹体全部被磨碎。

(4)提取次数:将上述已经研磨好的样品用超纯水超声波洗涤抽滤样品 5 次(每次 6 mL),可以较为完全地提取流体包裹体液相。提取后的石英样品置于瓷皿中,于 80℃烘干。

(5)样品溶解:将上述已经烘干的样品加入 HNO_3 和 HF 进行第一步溶样,大约 1 g 样品加入 0.5 mL HNO_3+5 mL HF,溶样时先加入 HNO_3,后加入 HF。其余溶样步骤参照苏嫒娜等(2011)和 Tian Shihong 等(2012)。纯化后样品进行 MC-ICP-MS 测试,即可得到石英流体包裹体和石英的 Li 同位素比值。

2 建立了适用于西藏本地岩石成因研究的 Li 同位素地质端元

最新地球物理和岩石学研究表明,印度下地壳在早—中中新世俯冲到拉萨地块之下(Searle et al., 2011; Shi Danian et al., 2015; Xu Qiang et al., 2015; Tian Shihong et al., 2017a, 2020a, b)。中拉

萨地块是由元古代和太古代结晶基底构成的微大陆(Zhu Dicheng et al., 2009,2011,2013),而其南北两侧均显示了新生下地壳的特征(Zhu Dicheng et al., 2011; Hou Zengqian et al., 2015a)。因此,印度—亚洲俯冲带的岩石圈结构异常复杂,目前地球化学 Li 同位素储库难以解释青藏高原富钾岩石 Li 同位素的组成(Tian Shihong et al., 2020a)。传统上只有地幔(Tomascak and Langmuir, 1999; Krienitz et al., 2012; Tomascak et al., 2016; Penniston-Dorland et al., 2017)、大陆上中下地壳(Teng Fangzhen et al., 2004, 2008, 2009; Sauzéat et al., 2015; Tomascak et al., 2016; Penniston-Dorland et al., 2017)的 Li 同位素组成,亦缺乏新生下地壳的 Li 同位素组成(Teng Fangzhen et al., 2007),无法识别是印度(上)地壳、印度下地壳、新生下地壳还是拉萨地块本身基底物质参与了青藏高原富钾火山岩、斑岩等岩石类型的形成。由于在玄武岩的形成和分异过程中,Li 同位素不发生有意义的分馏(Tomascak et al., 1999a),Teng Fangzhen 等(2007)认为新生地壳和地幔应该具有相同的 Li 同位素组成。尤其是,传统的大陆下地壳的 δ^7Li 值变化非常大(-14.0‰~+14.3‰),囊括了拉萨地块富钾火山岩的 Li 同位素组成(Tian Shihong et al., 2020a),无法进行相关解释。因此,解决上述岩石成因模型,关键在于能否找到适用于西藏本地岩石成因研究的各种 Li 同位素地质端元(比如印度上下地壳、新生下地壳、拉萨上下地壳、地幔等)。根据各地质端元样品的岩石地球化学和 Sr—Nd—Pb—Hf—O 同位素特征,首先选定能代表相应地质端元的岩石样品,再分析这些样品的 Li 同位素组成,从而建立青藏高原主要地质端元的 Li 同位素储库。因此,实际上是建立不同地质端元的多元同位素示踪体系,相互印证,确保所建立的 Li 同位素储库可靠性。研究团队优先确定了印度上下地壳和新生下地壳的 Li 同位素组成(Tian Shihong et al., 2017b,2018),也确定了印度下地壳的 Mg 同位素组成(Tian Shihong et al., 2020b)。

根据全岩主量元素、微量元素和 Sr—Nd—Pb 同位素数据,认为洛扎、隆子淡色花岗岩代表了印度上地壳组成,而打拉和确当二云母花岗岩以及聂拉木麻粒岩和片麻岩代表了印度下地壳组成。印度上地壳 Li 含量为 23~45 μg/g,平均值为 34 μg/g,与大陆上地壳 Li 含量加权平均值相一致(35±11 μg/g)。印度下地壳 Li 含量为 33~84 μg/g,平均值为 58 μg/g,远高于大陆下地壳的平均 Li 含量(约 8 μg/g),这与黑云母和白云母含量高有关。与大陆上地壳平均 Li 同位素组成相比(0±2‰; Teng Fangzhen et al., 2004),印度上地壳 Li 同位素组成相对偏重(+0.9‰~+5.6‰)。而印度下地壳的 Li 同位素组成(-4.4‰~-0.1‰)明显轻于印度上地壳的 Li 同位素组成(+0.9‰~+5.6‰),其范围比大陆下地壳的更为有限(-14.0‰~+14.3‰; Teng Fangzhen et al., 2008)。印度上地壳高的 δ^7Li 值是由于印度下地壳释放的高 δ^7Li 流体造成的,而印度下地壳低的 δ^7Li 值是由于残余印度下地壳部分熔融形成的。因此,Li 同位素是区分喜马拉雅地区淡色花岗岩和二云母花岗岩源区的有效手段(Tian Shihong et al., 2017b)。此外,认为聂拉木和东喜玛拉雅构造结麻粒岩、角闪岩和片麻岩代表了印度下地壳组成,其 δ^{26}Mg 分别为-0.44‰~-0.09‰、-0.44‰~-0.10‰和-0.70‰~-0.03‰。因此,印度下地壳的 Mg 同位素组成为-0.70‰~-0.03‰(Tian Shihong et al., 2020b),位于大陆下地壳的 Mg 同位素组成范围内(-0.70‰~+0.19‰; Teng Fangzhen et al., 2013)。

根据全岩主量元素、微量元素和 Sr—Nd—Pb 同位素数据,认为叶巴组玄武岩和冈底斯辉长岩是交代岩石圈地幔部分熔融的产物,成分上与新生下地壳相似。而典中组安山岩和冈底斯闪长岩则是新生下地壳部分熔融形成的。因此,这些样品代表了新生下地壳的组成。新生下地壳 Li 含量为 7.1~37.2 μg/g(平均值为 15.4 μg/g),与大陆下地壳 Li 含量相一致(13 μg/g);Li 同位素组成为+0.8‰~+6.6‰(平均值为 3.0‰),与 EMI/EMII 地幔的相似。新生下地壳的 Li 同位素组成归因于大陆岩石圈地幔的部分熔融,受到俯冲洋壳和沉积物的不同比例流体的交代。该研究成果亦证实新生下地壳和交代岩石圈地幔具有一致的 Li 同位素组成,说明在玄武岩浆底侵和结晶分异期间,未发生 Li 同位素分馏(Tian Shihong et al., 2018)。

3　Li 同位素地质应用

3.1　青藏高原岩石圈结构及其隆升历史

青藏高原的逐渐隆升影响了新生代亚洲季风和干旱化的格局,甚至全球气候(Chung et al., 1998; Dupont-Nivet et al., 2007; Shen Xingyan et al., 2017)。隆升的历史和机制是理解这些现象的关键因素。几种构造模型来解释青藏高原的形成,包括 Argand-type 俯冲(Argand, 1924)、活动地块的侧向

挤出(Molnar and Tapponnier,1975)、向南俯冲和回转(Willett and Beaumont,1994)、板内俯冲(Kosarev et al., 1999)、下地壳隧道流(Beaumont et al., 2001)和地壳流(Chen Lin et al., 2017)等。尽管并不清楚是印度地壳的哪部分(印度上地壳或印度下地壳)参与了高原隆升(Nábělek et al., 2009; Copley et al., 2011; Searle et al., 2011; Shi Danian et al., 2015; Xu Qiang et al., 2015; Tian Shihong et al., 2017a),但通常认为印度陆壳俯冲解释了青藏高原的形成(Copley et al., 2011; Shi Danian et al., 2015)。青藏高原广泛分布的火山岩和侵入岩为研究西藏隆升历史及相关深部地球动力学过程提供了很好的研究对象(Guo Zhengfu et al., 2006; Wang Qiang et al., 2008; Chen Jianlin et al., 2017; Ou Quan et al., 2017)。然而,它们的成因仍有争议。已有的研究模型,包括加厚下地壳(Chen Jianlin et al., 2010; Liu Dong et al., 2014,2017; Ou Quan et al., 2017)、拆层下地壳(Chen Jianlin et al., 2013)或俯冲陆壳(Wang Qiang et al., 2008; Lai Shaocong and Qin Jiangfeng,2013)的部分熔融和交代岩石圈地幔的低度部分熔融(Miller et al., 1999; Jiang Yaohui et al., 2006; Zhao Zhidan et al., 2009; Huang Feng et al., 2015; Liu Dong et al., 2015)。该岩石圈地幔可能受来自俯冲的特提斯大洋板块(Gao Yongfeng et al., 2009; Tommasini et al., 2011; Liu Dong et al., 2015)、印度陆壳(Zhao Zhidan et al., 2009; Cheng Zhihui and Guo Zhengfu, 2017; Zhang Lihong et al., 2017)或印度下地壳(Guo Zhengfu et al., 2015; Tian Shihong et al., 2017a)的流体/熔体交代。针对这些科学问题,Li—Mg 同位素能够为火山岩成因提供新的约束:① Li 和 Mg 在高温岩浆过程中同位素分馏作用有限,而在低温过程中表现出较大的同位素分馏(Tomascak et al., 2016; Teng Fangzhen et al., 2017)。例如,低温蚀变洋壳具有重的 Li(δ^7Li 高达+14‰; Chan et al., 1992, 2002)和 Mg(δ^{26}Mg 高达+0.21‰; Liu Pingping et al., 2017; Huang Kangjun et al., 2018)同位素组成,这种蚀变洋壳脱水可产生具有重的 Li 和 Mg 同位素组成的流体(Chan and Kastner,2000; Simons et al., 2010; Chen Yixiang et al., 2016; Teng Fangzhen et al., 2016)。相比之下,化学风化作用更容易在大陆地壳中富集较重的 Mg 同位素组成(Li Wangye et al., 2010; Huang Kangjun et al., 2013; Yang Wei et al., 2016)和较轻的 Li 同位素组成(Teng Fangzhen et al., 2004,2008)。② 俯冲沉积物的 Li 和 Mg 同位素组成和含量差异明显(Bouman et al., 2004; Chan et al., 2006; Hu Yan et al., 2017)。例如,富含粘土的陆源沉积物具有低的 δ^7Li 值(低至-2‰)和高的 Li 含量(高达 79 μg/g)(Bouman et al., 2004; Chan et al., 2006);而沉积碳酸盐岩具有高的 δ^7Li 值和极低的 Li 含量(You and Chan,1996; Hall et al., 2005)。而富含粘土的陆源沉积物具有相对重的 δ^{26}Mg 值(Hu Yan et al., 2017),而沉积碳酸盐岩具有低的、变化范围大的 δ^{26}Mg(-5.6‰~-0.6‰)和 MgO 含量(高达 23%)(Saenger and Wang Zhengrong, 2014; Teng Fangzhen et al., 2017)。③ 建立了地幔、地壳和水圈的 Li—Mg 同位素储库(Tomascak et al., 2016; Teng Fangzhen et al., 2017),尤其是建立了适用于西藏本地岩石成因研究的 Li—Mg 同位素地质端元(Tian Shihong et al., 2017b,2018,2020b)。因此,Li 和 Mg 同位素与传统的 Sr—Nd 同位素相结合,可以很好地解译青藏高原火山岩的岩石成因以及与俯冲相关的地质作用过程,如熔流体交代作用。

3.1.1 印度下地壳俯冲到拉萨地块之下的 Li 同位素证据

普遍认为超钾质(UPV; MgO>3%, K_2O>3%, K_2O/Na_2O>2)和富镁钾质(MPR; MgO≥6%, K_2O/Na_2O≥1)火山岩来自于交代岩石圈地幔的部分熔融(Miller et al., 1999; Zhao Zhidan et al., 2009; Huang Feng et al., 2015; Liu Dong et al., 2015),而钾质火山岩(PVR)来自于西藏加厚下地壳的部分熔融(Chen Jianlin et al., 2010; Liu Dong et al., 2014,2017)。据此,Tian Shihong 等(2020a)对拉萨地块 87 件钾质岩、超钾质岩和富镁钾质岩进行了 Li 含量和同位素组成分析,并结合新的 Pb—Sr—Nd 同位素数据和全岩分析,对其地幔来源和岩石成因进行了约束。这些岩石的 δ^7Li 值非常相似:钾质岩 δ^7Li 为-4.9‰~+3.2‰,超钾质岩 δ^7Li 为-3.9‰~+1.7‰,富镁钾质岩 δ^7Li 为-1.2‰~+3.5‰。将其分为两组(图 5):第一组(19 件)具有重的 δ^7Li 值(+1.0‰~+3.5‰),类似于洋中脊和洋岛玄武岩的 Li 同位素组成;第二组(68 件)具有轻的 δ^7Li 值(-4.9‰~+1.0‰),类似于印度下地壳的 Li 同位素组成(Tian Shihong et al., 2017b)。这些变化的 Li 同位素组成不是扩散同位素分馏或俯冲洋壳脱流体造成的,而是记录了早—中中新世大陆岩石圈地幔的同位素特征,拉萨地块之下存在轻 δ^7Li 地幔区,

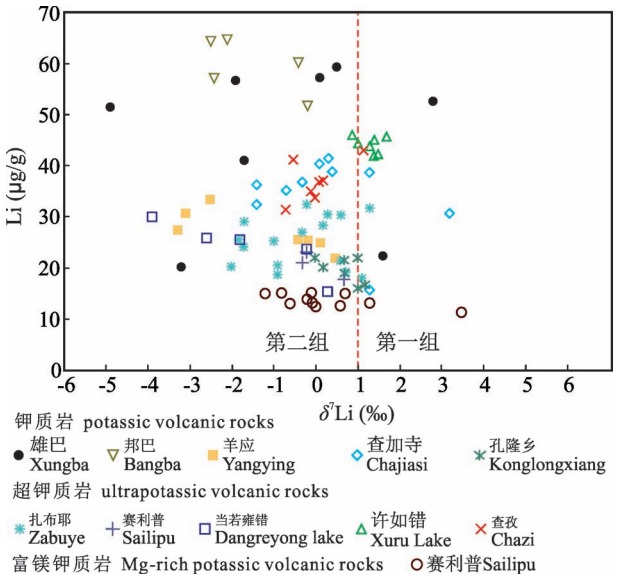


图 5 拉萨地块钾质岩、超钾质岩和富镁钾质岩 δ^7Li—Li 关系图解(据 Tian Shihong et al., 2020a)

Fig. 5 Li versus δ^7Li diagram for the potassic, ultrapotassic and Mg-rich potassic volcanic rocks in Lhasa terranes (from Tian Shihong et al., 2020a)

可能是上覆岩石圈地幔先后经历了来自印度下地壳富δ^7Li 流体交代和脱水印度下地壳贫δ^7Li 熔体交代。印度下地壳与交代岩石圈地幔的模拟计算可以解释钾质岩、超钾质岩和富镁钾质岩的成分变化。这三套岩石是大陆岩石圈地幔部分熔融形成的,该地幔受到俯冲印度下地壳熔流体的交代,交代比例分别为 4%~14%、4%~10%和 6%~10%(图 6)。Li 同位素数据指示印度下地壳俯冲到中拉萨地块之下(图 7),从而为青藏高原的形成提供了新证据。

此外,通过对喜马拉雅麻粒岩、角闪岩和片麻岩以及中新世淡色花岗岩和始新世二云母花岗岩的 Mg 同位素系统对比研究,发现印度下地壳俯冲到喜马拉雅之下(Tian Shihong et al., 2020b),进而往北俯冲到中拉萨地块之下(Tian Shihong et al., 2020a),造成了青藏高原的隆升。

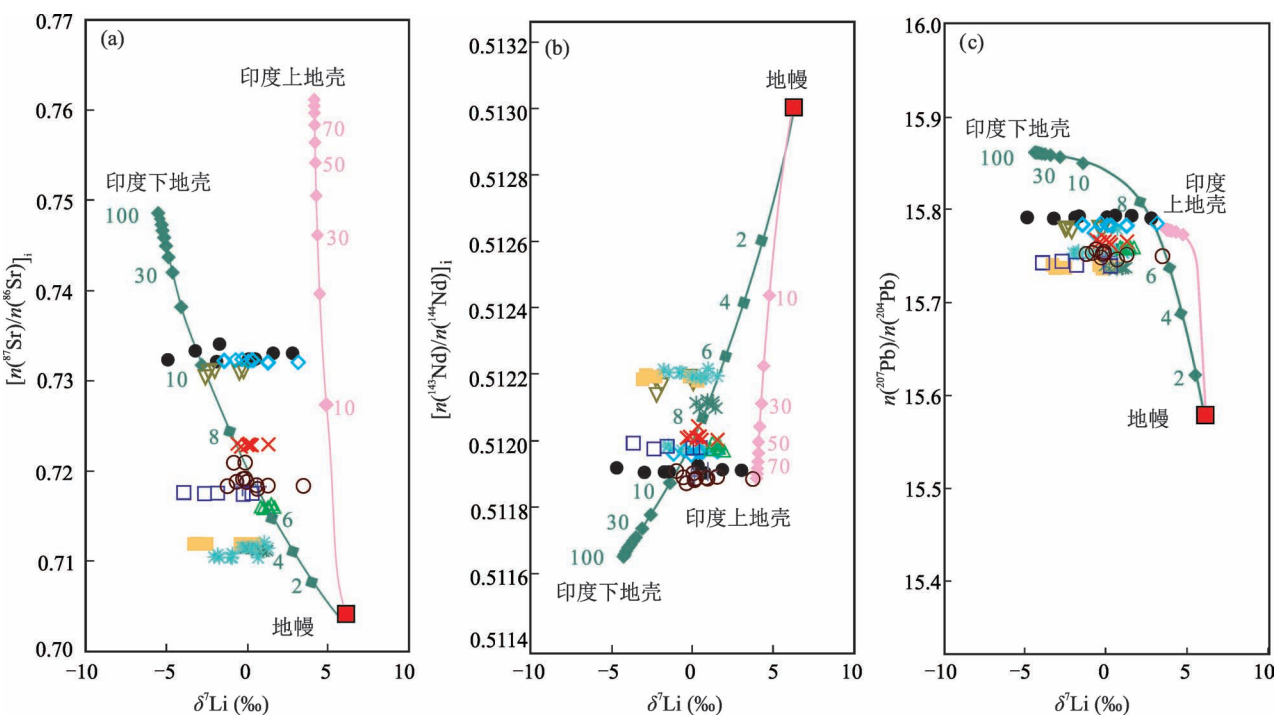


图 6 拉萨地块钾质岩、超钾质岩和富镁钾质岩 δ^7Li—□$n(^{87}Sr)/n(^{86}Sr)$□$_i$、δ^7Li—□$n(^{143}Nd)/n(^{144}Nd)$□$_i$ 和 δ^7Li—$n(^{207}Pb)/n(^{204}Pb)$ 图解(据 Tian Shihong et al., 2020a)。地幔和印度上下地壳的 Li 同位素值来自 Tian Shihong 等(2017b, 2018);图例同图 5

Fig. 6 δ^7Li values compared with □$n(^{87}Sr)/n(^{86}Sr)$□$_i$, □$n(^{143}Nd)/n(^{144}Nd)$□$_i$, $n(^{207}Pb)/n(^{204}Pb)$ ratios for the potassic, ultrapotassic and Mg-rich potassic volcanic rocks in Lhasa terranes (from Tian Shihong et al., 2020a). δ^7Li values of the mantle, Indian lower crust and Indian upper crust end-member components are from Tian Shihong et al. (2017b, 2018); symbols are as in Fig. 5

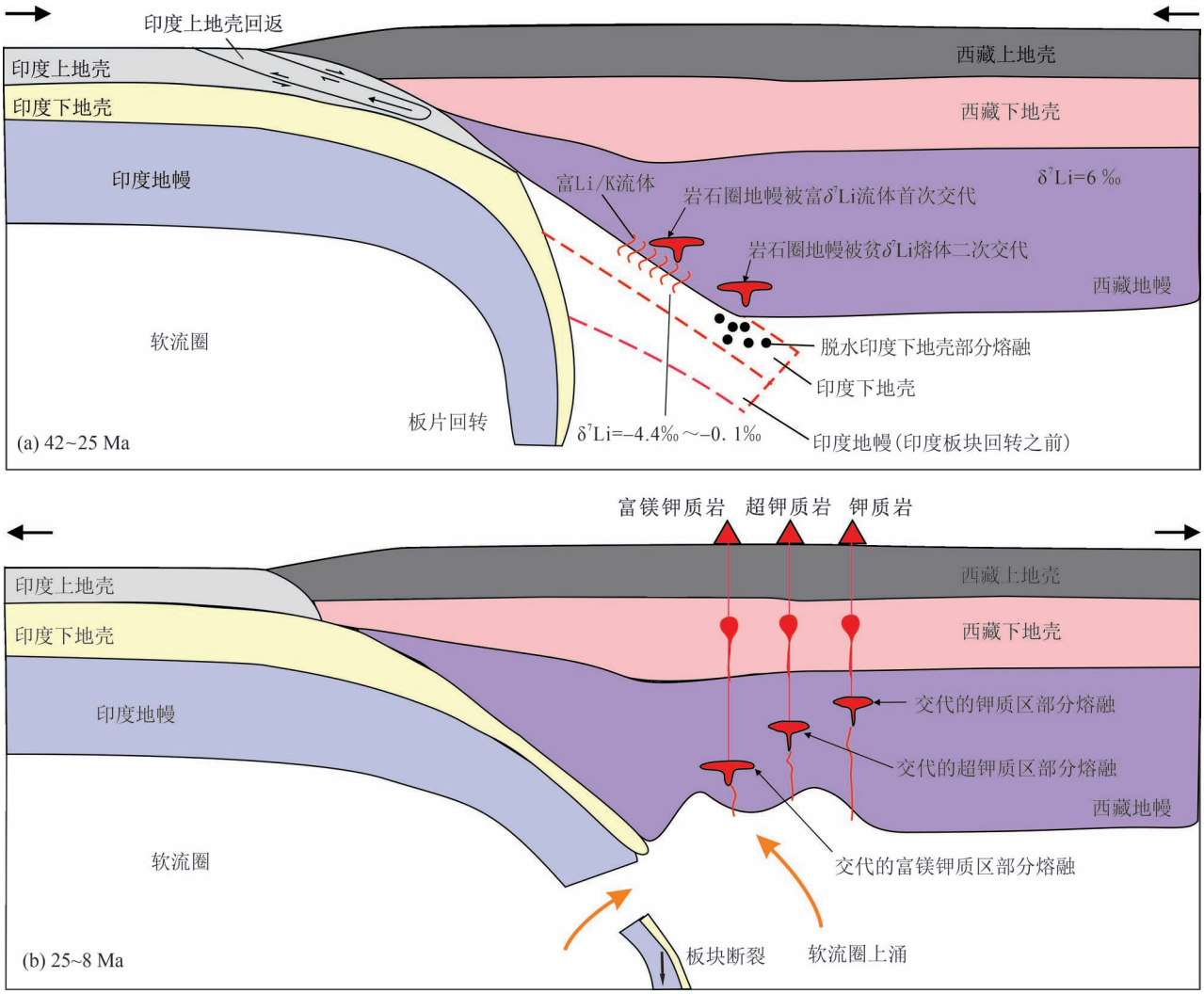


图 7 拉萨地块钾质岩、超钾质岩和富镁钾质岩形成示意图(据 Tian Shihong et al., 2020a)

Fig. 7 A sketch map showing the formation of the the potassic, ultrapotassic and Mg-rich potassic volcanic rocks in Lhasa terranes(from Tian Shihong et al., 2020a)

3.1.2 青藏高原中部存在残余大洋板块的 Li—Mg 同位素证据

地球物理研究表明,向北俯冲的印度板块和特提斯板块没有到达羌塘地块的南部边界(Owens and Zandt,1997; Tilmann et al., 2003)。相反,松潘—甘孜地体已经俯冲到羌塘块体之下(Tapponnier et al., 2001; Ding Lin et al., 2007)。这种俯冲作用将对青藏高原火山岩成因和地表隆升产生深远的影响。然而,羌塘地区广泛存在的后碰撞火山岩普遍认为有几种不同的成因,包括加厚的(Ou Quan et al., 2017)、拆沉的(Chen Jianlin et al., 2013)或俯冲大陆地壳(Wang Qiang et al., 2008; Lai Shaocong and Qin Jiangfeng,2013)的部分熔融。这些不同解释阻碍了对深部地球动力学过程的清晰理解。据此,Tian Hengci 等(2020)对羌塘北部的多彩玛和那日尼亚两套火山岩的全岩 Sr—Nd—Mg—Li 同位素和锆石 U-Pb 年龄进行了综合研究。多彩玛高钾钙碱性粗安岩形成于 35 Ma 左右,富集稀土元素和大离子亲石元素,具有低的 $\delta^{26}Mg$(-0.41‰~-0.33‰)和 $\delta^{7}Li$(+1.0‰~+2.6‰)值。结合高的 $n(^{87}Sr)/n(^{86}Sr)_i$(0.7066~0.7067)和低 $\varepsilon_{Nd}(t)$(-1.96~-1.61)特征,多彩玛粗安岩最有可能来源于先前受俯冲富镁碳酸盐岩沉积物(比如白云石)熔体交代的岩石圈地幔(图 8)。模型计算表明 7%~11%的富镁碳酸盐岩沉积物通过熔融方式加入到地幔中。相比之下,同期的那日尼亚埃达克质(高锶低钇)粗面岩具有高的 $\delta^{26}Mg$(-0.13‰~-0.02‰)和 $\delta^{7}Li$(+3.3‰~+5.4‰)值,以及高 Pb/

Ce 和 Ba/La 值,这最有可能来源于受松潘—甘孜大洋板片释放的流体交代的加厚下地壳(图 8)。

基于发育于北羌塘地区的埃达克质岩石和岩脉的岩石成因,前人认为藏中地区早在 45~38 Ma 就开始隆升(Wang Qiang et al., 2008; Chen Jianlin et al., 2013; Ou Quan et al., 2017)。通过对那日尼亚和多采玛岩石的锆石 U-Pb 年龄研究,认为在 38 Ma 存在残余大洋板块,说明松潘—甘孜地体的俯冲速度较之前的估计要慢。松潘—甘孜和羌塘碰撞所引起的地壳增厚会导致那日尼亚地区地表隆升。因此,那日尼亚火山岩的年龄为西藏中部地表隆升的时间提供了重要的约束。基于地球化学观测的构造重建表明,西藏中部的隆升可能在~38 Ma 之前轻微启动,可能比之前认为的要晚(Wang Qiang et al., 2008; Chen Jianlin et al., 2013)。这一解释也支持了最近的观点,即青藏高原中部始新世古海拔(约 1000 m; Sun Jimin et al., 2014; Botsyun et al., 2019)比之前估计的要低(Rowley and Currie, 2006)。

3.2　川西碳酸岩型稀土矿床富集机制

岩浆碳酸岩一直是岩石学界研究热点之一,这不仅是因为碳酸岩来源于深部地幔(富集地幔和/或软流圈)而作为大陆地幔地球化学的"探针岩石"来了解地幔组成与演化、地幔交代作用与不均一性以及岩浆形成的动力学背景(Hou Zengqian et al., 2006; Halama et al., 2007, 2008; Cheng Zhiguo et al., 2017; Doroshkevich et al., 2017; Cheng Zhiguo et al., 2018; Su Jianhui et al., 2019),而且因为其多伴生重要的 REE—Nb—Ta—Fe 金属矿化而具有重要的理论和实际意义(Hou Zengqian et al., 2009, 2015b; Xie Yuling et al., 2016; Liu Yan and Hou Zengqian, 2017; Xie Yuling et al., 2019; Yang Kuifeng et al., 2019)。尽管前人在碳酸岩研究方面取得了很多重要的研究成果,但研究的构造背景主要集中于大陆裂谷环境,即由非造山作用引起的大地构造背景,而对于碰撞造山带中的碳酸岩则很少研究(Le Bas, 1989; Tilton et al., 1998)。通常认为裂谷环境碳酸岩是由地幔柱活动引起的次岩石圈地幔部分熔融而形成的(Bell and Simonetti, 2010)。Halama 等(2007, 2008)研究发现裂谷环境碳酸岩及其伴生硅酸盐的 Li 同位素组成为+4‰±2‰(图 9b),而未见碰撞环境碳酸岩和伴生硅酸盐的 Li 同位素数据有关报道。据此,Tian Shihong 等(2015)首次报道了印度—亚洲碰撞带东缘冕宁—德昌稀土成矿带的牦牛坪、里庄和大陆槽 38 件碳酸岩和正长岩的 Li 含量和同位素组成,结合 Pb—Sr—Nd—C—

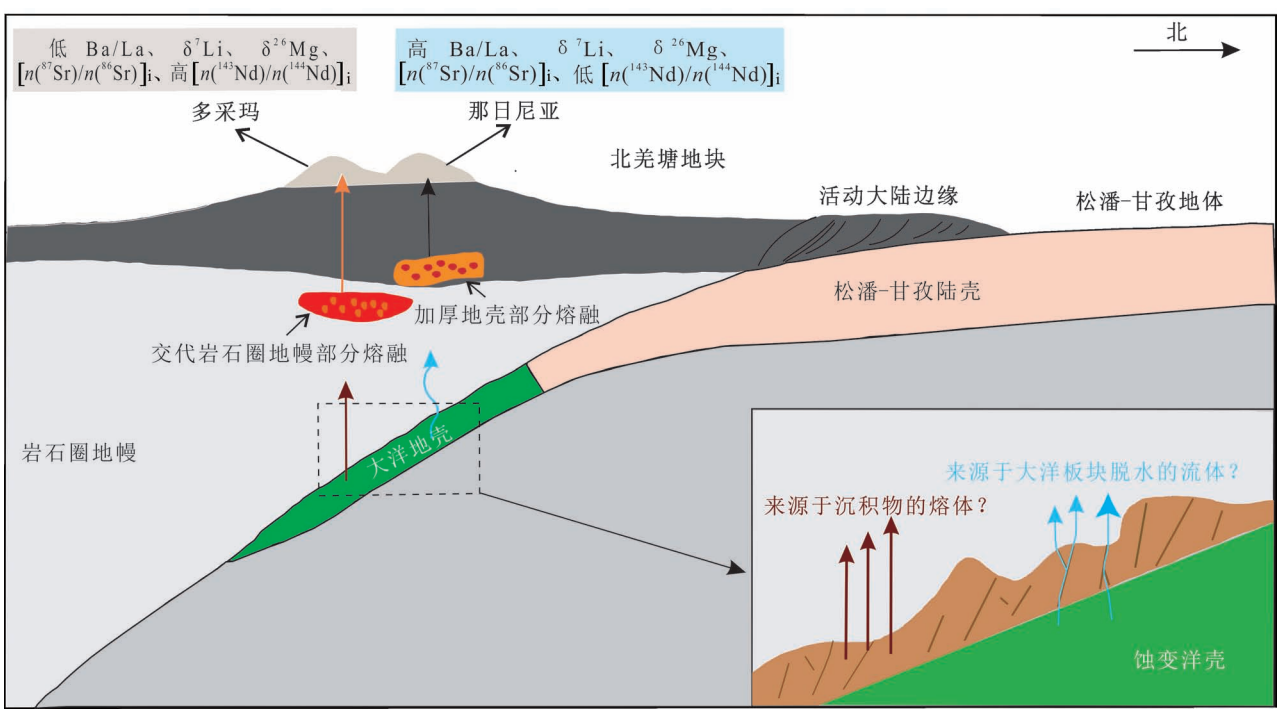


图 8 北羌塘地块那日尼亚埃达克质(高锶低钇)粗面岩和多采玛粗安岩形成示意图(据 Tian Hengci et al., 2020)

Fig. 8 A sketch map showing the formation of the Nariniya adakitic trachytes and Duocaima trachyandesites in North Qiangtang terranes(from Tian Hengci et al., 2020)

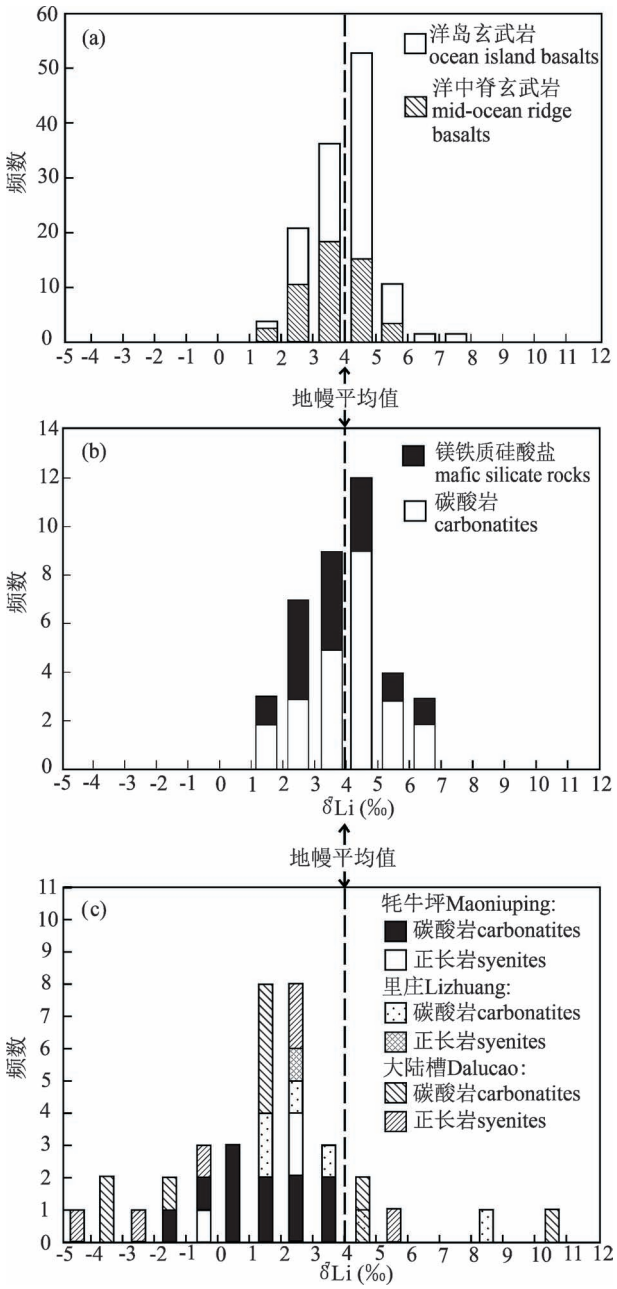


图 9 δ^7Li 值频率分布图:(a)洋岛玄武岩和洋中脊玄武岩;(b)裂谷环境碳酸岩和硅酸盐;(c)川西碳酸岩和正长岩。虚线代表地幔平均值(+4‰)(据 Tian Shihong et al., 2015)

Fig. 9 Frequency distribution diagrams of δ^7Li values for (a) OIB and MORB; (b) carbonatites and mafic silicate rocks in rift zones; and (c) carbonatites and syenites in western Sichuan. The dashed line indicates the average mantle value of ~+4‰ (from Tian Shihong et al., 2015)

O 同位素和全岩分析数据,对这些碳酸岩浆的源区性质和岩石成因以及与印度—亚洲大陆碰撞有关的壳幔相互作用过程提供了新的制约。

川西碳酸岩和正长岩的 Li 含量和同位素组成分别为 0.8~120 μg/g 和-4.5‰~+10.8‰(图 9c),变化范围均很大。其中,大多数碳酸岩和正长岩的 δ^7Li 值为+0.2‰~+5.8‰,与 MORB 和 OIB 的相类

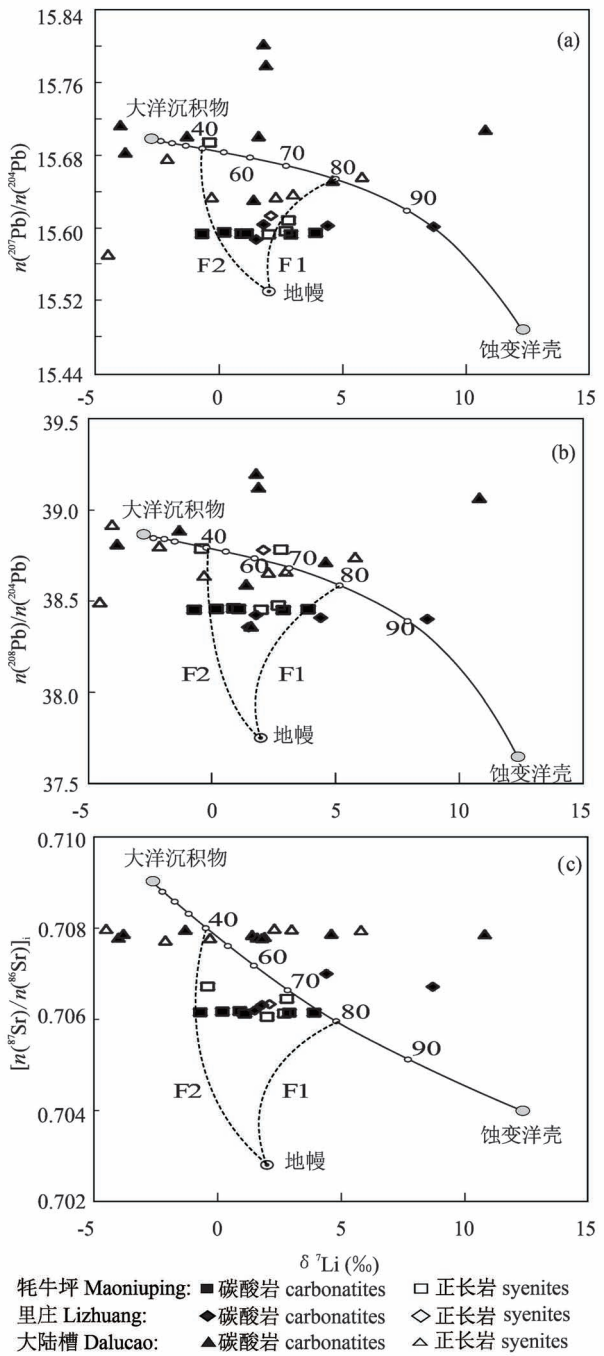


图 10 川西碳酸岩和正长岩 δ^7Li—$n(^{207}Pb)/n(^{204}Pb)$、δ^7Li—$n(^{208}Pb)/n(^{204}Pb)$ 和 δ^7Li—$n(^{87}Sr)/n(^{86}Sr)_i$,模拟图解(据 Tian Shihong et al., 2015)

Fig. 10 Diagrams showing variations in δ^7Li compared to $n(^{207}Pb)/n(^{204}Pb)$, $n(^{208}Pb)/n(^{204}Pb)$, and $n(^{87}Sr)/n(^{86}Sr)_i$, values for carbonatites and syenites in western Sichuan (from Tian Shihong et al., 2015)

似;3 件碳酸岩 δ^7Li 值较高,为+8.7‰~+10.8‰;5 件碳酸岩和 4 件正长岩的 δ^7Li 值较低,为-4.5‰~-0.3‰。这些变化大的 δ^7Li 值不是动力学分馏造成的,而是反映了新元古代大陆岩石圈地幔的同位素组成。碳酸岩的 Li 同位素组成变化范围大,暗示了古老岩石圈地幔存在异常的δ^7Li 组成。模拟计算表明,碳酸岩异常的δ^7Li 来源于大陆岩石圈地幔,受到俯冲洋壳和沉积物的不同比例流体的交代(AOC_{80}—SED_{20} to AOC_{40}—SED_{60};图 10)。据此,认为元古代俯冲的洋壳和沉积物富 Li 流体交代大陆岩石圈地幔,形成交代富集的大陆岩石圈地幔,新生代软流圈上涌和始新世—渐新世减压熔融导致岩石圈地幔部分熔融,形成碳酸岩—正长岩母岩浆,两者发生液态不混溶作用,形成碳酸岩和正长岩。综上所述,裂谷环境碳酸岩来源于次岩石圈地幔(与地幔柱有关),未受到俯冲作用和地壳循环的影响,其 δ^7Li 值为+4±2‰(Halama et al., 2007,2008);碰撞环境碳酸岩来源于大陆岩石圈地幔,受到洋壳和沉积物流体的交代作用,其 δ^7Li 值为-4.5‰~+10.8‰(Tian Shihong et al., 2015)。该成果与 Hou Zengqian 等(2015)观点不谋而合,认为大洋沉积物参与了碳酸岩型稀土矿床的形成。此外,Li 同位素提供了一种鉴别裂谷环境与碰撞环境碳酸岩和研究地壳循环的有效方法。

3.3　四川呷村 VMS 型矿床成矿流体来源

火山成因块状硫化物(VMS)矿床,也称为以火山岩为容矿岩石的块状硫化物(VHMS)矿床。由于其成因不仅涉及到成矿学的一般理论问题,而且涉及到岩石圈/水圈/生物圈的相互作用,因此,一直是国际成矿学界的研究热点(Yang Kaihui and Scott, 2002; Franklin et al., 2005)。为此,Yang Dan 等(2015)选择我国最典型的 VMS 矿床——四川呷村大型铅锌铜多金属矿床(侯增谦等,2001),在研发了石英 Li 同位素分析方法基础上,重点针对成矿流体来源问题,系统开展了热液石英和流体包裹体的 Li—O 同位素地球化学研究。通过大量石英—流体包裹体 Li 同位素分析和均一温度测定,深入探讨了矿物—流体 Li 同位素分馏,建立了石英—流体 Li 同位素分馏经验公式:$\Delta\delta^7Li_{石英—流体} = -8.9382 \times (1000/T) + 22.22$(线性相关系数 $R^2 = 0.98$,175~340 ℃;图 11),为利用热液矿床广泛发育的热液石英示踪成矿流体来源奠定了重要基础;并首次将 Li 同位素用于矿床成矿流体研究中,获得了呷村矿床一批热液石英和流体包裹体的 Li 同位素分析数据,综合分析呷村矿床下覆脉状—网脉状矿带和上部块状矿体的 Li—O 同位素组成及其空间变化规律,定量估算了成矿流体中岩浆水—海水混合比例(图 12),提供了岩浆水大量参与成矿的Li同位素新证

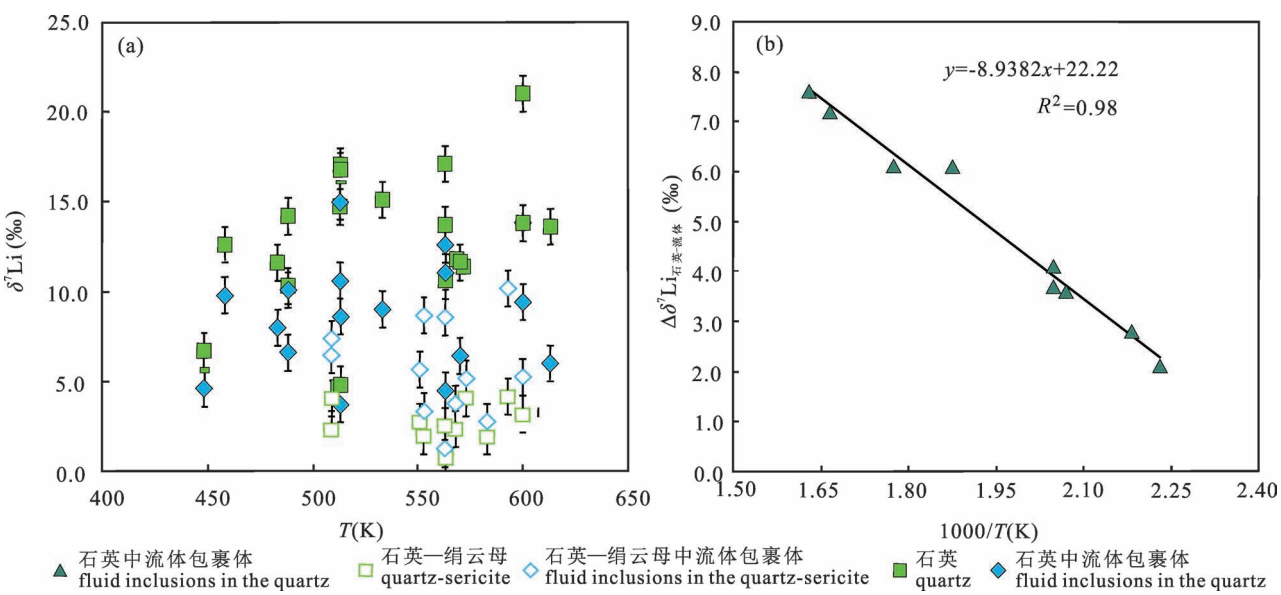
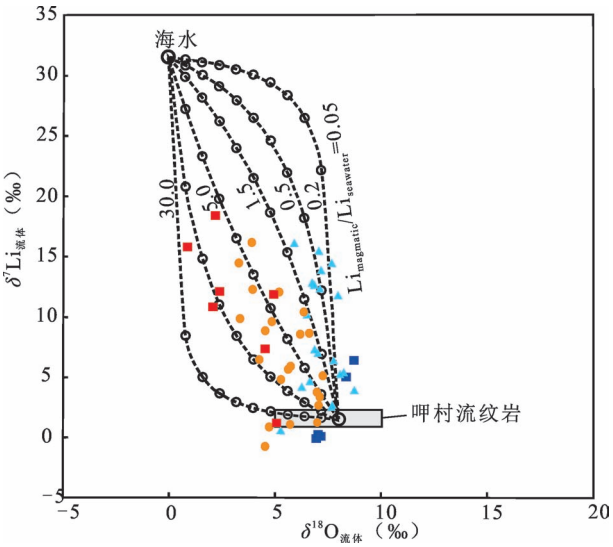


图 11 (a)石英和流体包裹体的 δ^7Li 随均一温度的变化图解;(b) 9 件纯石英中的流体包裹体 Li 同位素分馏系数($\Delta_{石英—流体}$)与均一温度(1000/T)的关系图解(据 Yang Dan et al., 2015)

Fig. 11 (a) Variation in δ^7Li of the host quartz and fluid inclusions with the measured homogeneous temperatures; (b) relationship of Li isotopic fractionation factor (Δquartz—fluid) with homogeneous temperatures (1000/T) of fluid inclusions hosted in nine pure-quartz samples (from Yang Dan et al., 2015)



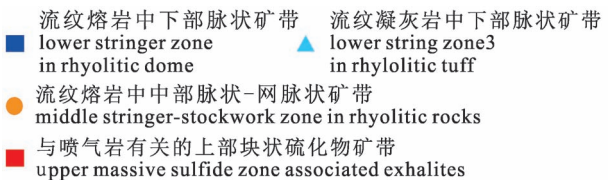


图 12 川西岬村矿床成矿流体 $\delta^7Li_{流体}$—$\delta^{18}O_{流体}$ 模拟图解，其中海水端元 $\delta^7Li = 31.5‰$，$\delta^{18}O = 0‰$，岩浆端元 $\delta^7Li = 1.5‰$，$\delta^{18}O = 8‰$（据 Yang Dan et al.，2015）

Fig. 12 Oxygen—lithium isotopic compositions of the ore-forming fluids at Gacun deposit, western Sichuan, which can be reproduced by mixing of variable amounts of seawater ($\delta^7Li = +31.5‰$, $\delta^{18}O = +0‰$) with a magmatic fluid ($\delta^7Li = +1.5‰$; $\delta^{18}O = +8‰$) with variable $Li_{magma}/Li_{sea\ water}$ mass mixing ratios (from Yang Dan et al., 2015)

据，再塑了两端元流体混合过程及其空间变化，完善了岬村矿床成矿模型（图 13）。

3.4 四川甲基卡硬岩型 Li 矿床富集机理

花岗伟晶岩是 Ta、Nb、Li、Cs 等稀有金属矿床的主要寄主岩（Lü Zhenghang et al., 2018; Ballouard

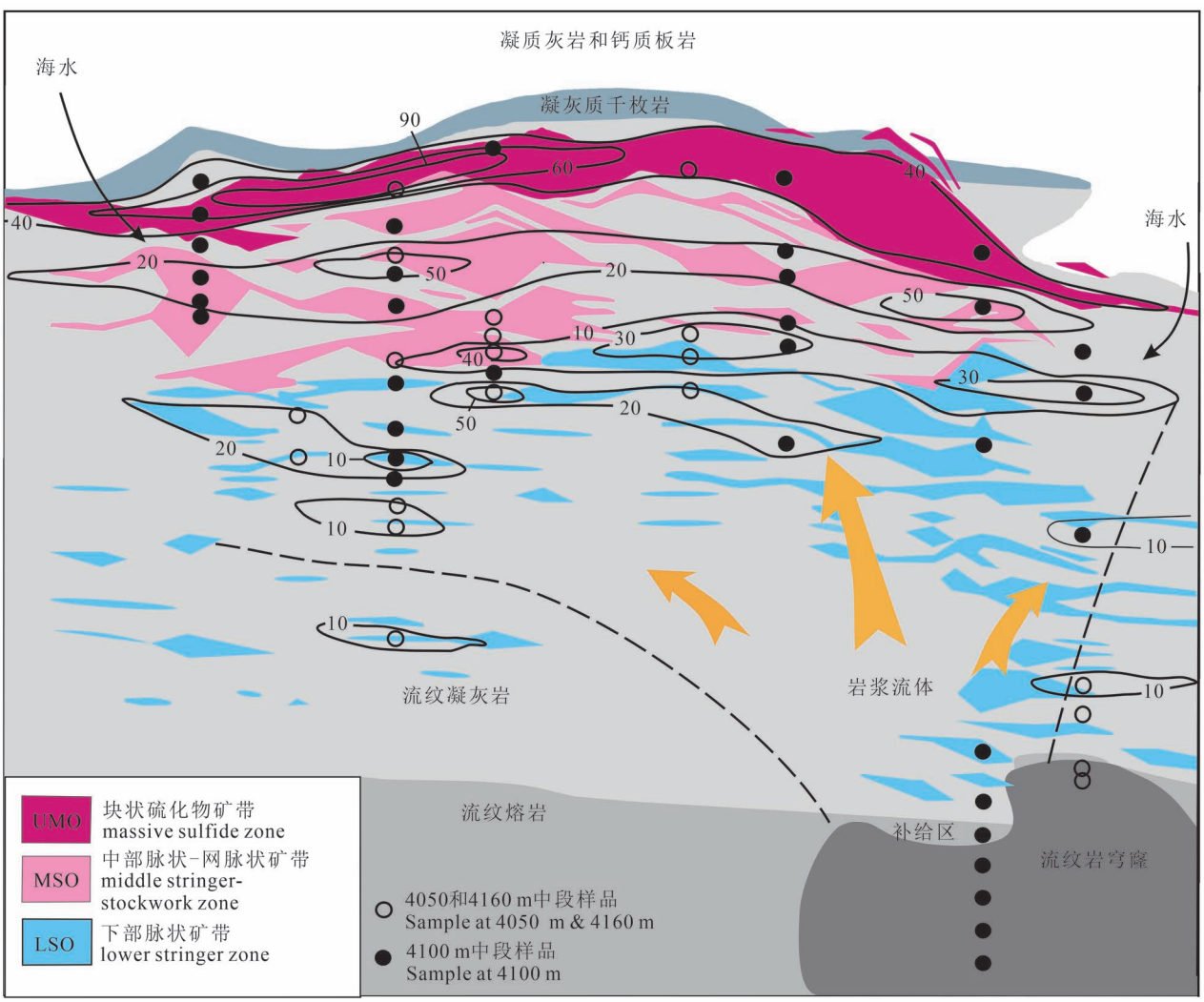


图 13 川西岬村矿床成矿流体中海水所占比例图（据 Yang Dan et al.，2015）

Fig. 13 Proportion diagram of sea water in the ore-forming fluids at Gacun deposit, Sichuan (from Yang Dan et al., 2015)

al.，2020),这些稀有金属对新技术和军事工业至关重要。然而,花岗伟晶岩的成岩成矿作用仍不清晰。通常认为伟晶岩是过铝质花岗岩浆极端分离结晶的最终产物(Teng Fangzhen et al.，2006a; Thomas and Davidson et al.，2012; Mulja and Williams-Jones,2018; Roda-Robles et al.，2018; 李贤芳等,2020)。这种分离结晶作用促进了残余熔体中稀有金属、助熔剂和挥发份的增加,进而导致花岗伟晶岩的发育和成矿。然而,对于一些研究程度高的伟晶岩,在其周围并未发现过铝质花岗岩,比如澳大利亚 Greenbush 伟晶岩、中国可可托海 3 号伟晶岩(Simmons and Webber,2008; Lü Zhenghang et al.，2018)。而且,在一些花岗—伟晶岩体系中,空间、时间和成分等存在不连续性。据此,一部分研究者认为伟晶岩来自相对低温下的变沉积岩的部分熔融(Simmons and Webber,2008; Martins et al.，2012; Deveaud et al.，2015; Müller et al.，2017; Gourcerol et al.，2019; Chen Bin et al.，2020; 刘涛等,2020)。该模式是基于直接的地壳深熔作用,导致伟晶岩浆中稀有金属富集的过程并不十分清楚,需要进一步调查研究(Thomas and Davidson et al.，2012; Deveaud et al.，2015)。另一些研究者认为来自硅酸盐熔体的超临界流体的出溶对花岗伟晶岩的成岩成矿作用具有重要指示意义(Thomas et al.，2009; Chakraborty and Upadhyay,2020; Fan Jingjing et al.，2020)。在花岗岩浆演化晚期,熔体—流体相互作用使岩浆分离成贫挥发份、富硅酸盐和富挥发份、贫硅酸盐(超临界流体)熔体体系。与残余硅酸盐熔体持续相互作用使出溶的超临界流体富含碱金属和助熔剂成分,导致稀有金属在花岗侵入体的

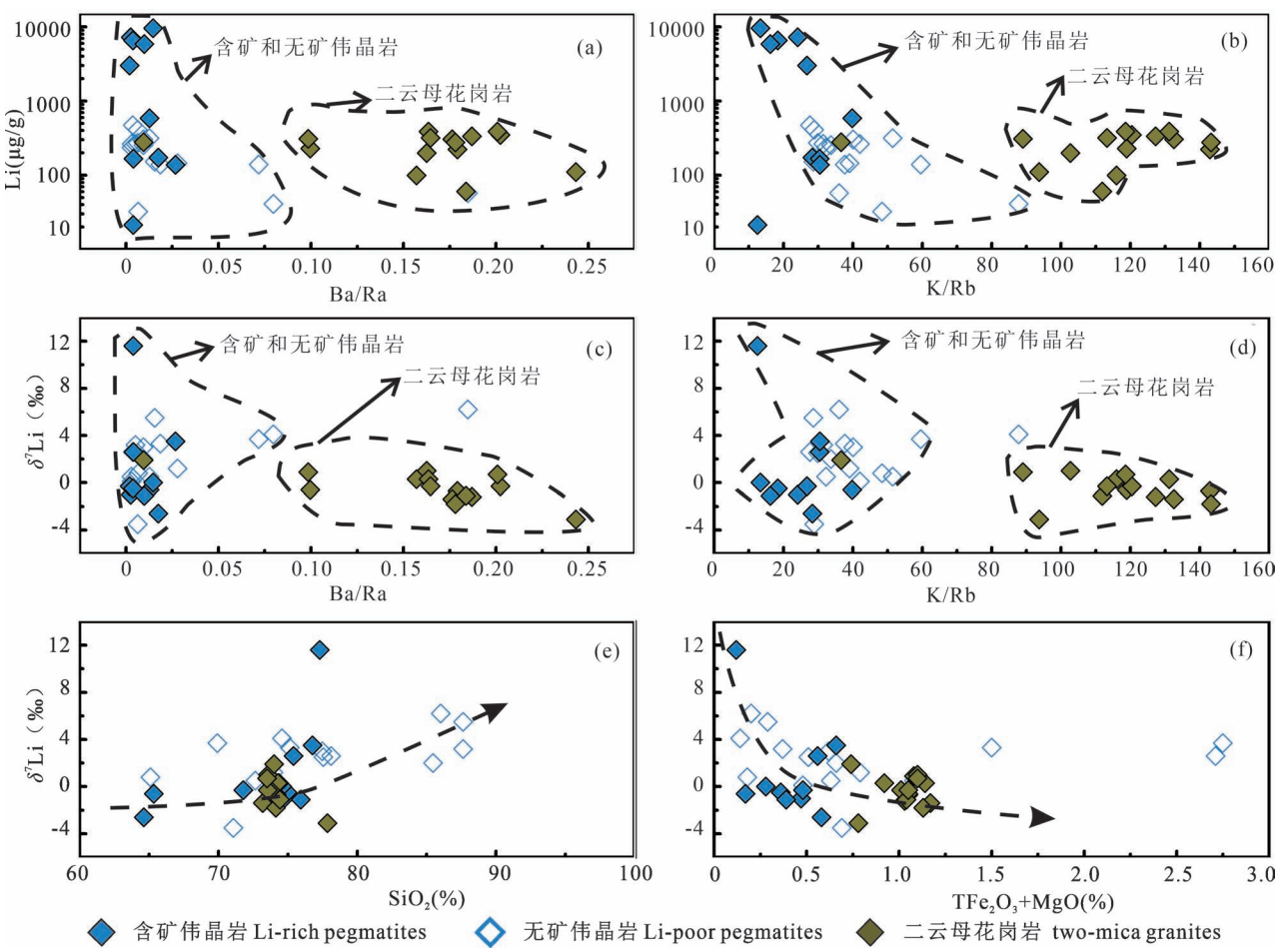


图 14 川西甲基卡二云母花岗岩、含矿伟晶岩和无矿伟晶岩相关图解:(a)Li—Ba/Rb、(b)Li—K/Rb、(c)δ^7Li—Ba/Rb、(d)δ^7Li—K/Rb、(e)δ^7Li—SiO_2 和(f)δ^7Li—TFe_2O_3+MgO(据 Zhang Huijuan et al.，2021)

Fig. 14 Diagrams showing variations in Li concentrations compared with (a) Ba/Rb and (b) K/Rb, and variations in δ^7Li compared with (c) Ba/Rb, (d) K/Rb, (e) SiO_2 and (f) TFe_2O_3+MgO (TFe_2O_3 = 0.8998×Fe_2O_3+ FeO) for Jiajika two-mica granites, Li-rich and Li-poor pegmatites in western Sichuan (from Zhang Huijuan et al.，2021)

内部和周围迁移,有利于形成花岗岩型或伟晶岩型稀有金属矿床(Thomas et al., 2009; Kaeter et al., 2018)。

四川甲基卡 Li 矿床含有高品位的稀有金属矿物,是中国最大的伟晶岩型 Li 矿床,其为研究花岗伟晶岩的成矿作用提供了一个天然实验室。尽管近年来做了很多研究工作(Li Jiankang et al., 2015; Li Jiankang and Chou I-Ming, 2016, 2017),但尚未完全理解甲基卡花岗伟晶岩的成矿作用。一种观点认为,伟晶岩是二云母花岗岩浆极端分离结晶的最终产物(Li Xianfang et al., 2020; Xu Zhiqin et al., 2020),其中结晶分异促进了残余熔体中不相容组份、助熔剂和挥发份的增加,进而引起稀有金属元素在花岗伟晶岩中聚集。另一种观点认为,花岗伟晶岩是在二云母花岗岩浆演化晚期期间流体/熔体不混溶的结果(London, 2018)。因此,有必要选择一种适合的示踪剂来探讨甲基卡花岗伟晶岩的成岩成矿作用。Li 同位素具有一些独特的地球化学性质,比如^{7}Li 和^{6}Li 质量差大(达 16.7%)导致了 Li 同位素在低温过程中可以产生大的同位素分馏(δ^{7}Li 值为-35‰~+50‰; Tomascak et al., 2016; Penniston-Dorland et al., 2017),以及强的流体活动性(You and Chan et al., 1996)等。这些特征使得 Li 同位素能示踪低温和高温环境中的各种地质过程,包括岩浆结晶分异、热液蚀变、熔体—流体相互作用以及稀有金属花岗—伟晶岩体系中的扩散(Richter et al., 2003; Teng Fangzhen et al., 2006a, 2006b; Deveaud et al., 2015; Tomascak et al., 2016; Penniston-Dorland et al., 2017; Li Jie et al., 2018; Ballouard et al., 2020; Chen Bin et al., 2020; Fan Jingjing et al., 2020)。据此,Zhang Huijuan 等(2021)首次系统报道了四川甲基卡 Li 矿床二云母花岗岩、含矿伟晶岩、无矿伟晶岩以及含矿和无矿伟晶岩中白云母的 Li 同位素组成数据,用以探讨岩浆结晶分异和流体出溶期间的 Li 同位素行为,进而探讨甲基卡矿床 Li 的富集机制及其超大型矿床的形成机理。

二云母花岗岩的平均 δ^{7}Li 值普遍低于含矿和无矿伟晶岩的 δ^{7}Li 值(图 14),而二云母花岗岩的 Li 含量(60.2~388 μg/g)与无矿伟晶岩(32.3~470 μg/g)基本相同,但远低于含矿伟晶岩(21.4~9584 μg/g)(图 14)。无矿伟晶岩中白云母的 Li 含量和 δ^{7}Li 值分别为 631~1265 μg/g 和-3.2‰~0,低于含矿伟晶岩中的白云母相应值(1221~1450 μg/g 和 0.1‰~2‰)(图 15)。所有这些数据显示,甲基卡

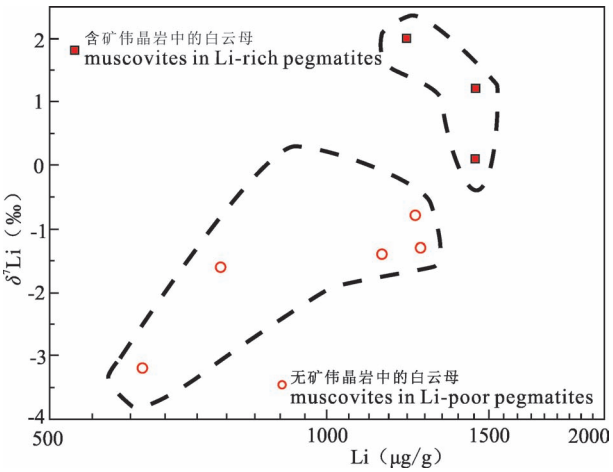


图 15 川西甲基卡含矿伟晶岩和无矿伟晶岩中白云母 δ^{7}Li—Li 相关图解(据 Zhang Huijuan et al., 2021)

Fig. 15 δ^{7}Li versus Li diagram for the muscovites from Jiajika Li-poor and Li-rich pegmatites in western Sichuan (from Zhang Huijuan et al., 2021)

花岗伟晶岩是二云母花岗岩浆极端分离结晶的产物,而并非直接深熔作用的结果,而且无矿伟晶岩从二云母花岗岩浆中优先分异出来,在岩浆结晶分异晚期再演化为含矿伟晶岩。相对于无矿伟晶岩,演化程度更高的含矿伟晶岩具有较低的 δ^{7}Li 值(图 14),可能是由于熔体—流体分离过程中流体出溶和动力扩散分馏导致的。研究发现熔体—流体分离过程中流体出溶会产生显著的 Li 同位素分馏,^{7}Li 富集于贫水富硅酸盐熔体中(图 16)。结合二云母

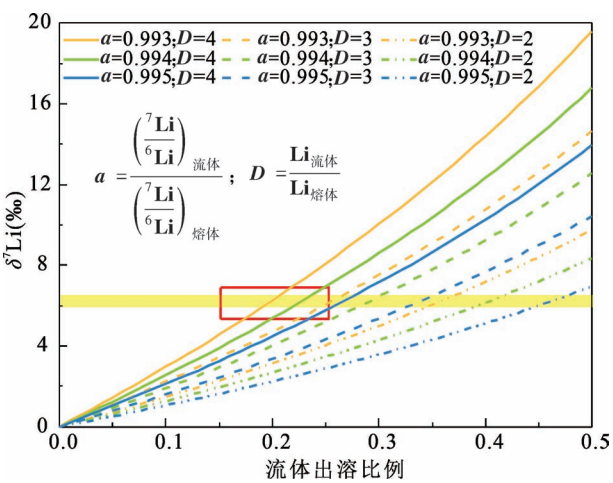


图 16 流体出溶过程中瑞利分馏模拟的 Li 同位素分馏(据 Zhang Huijuan et al., 2021)

Fig. 16 Li isotopic fractionation modeled by Rayleigh fractionation during fluid exsolution (from Zhang Huijuan et al., 2021)

花岗岩和花岗伟晶岩形成年龄以及其他地球化学证据,认为花岗岩浆演化末期的岩浆结晶分异和流体出溶以及富 Li 地层导致了 Li 的多期富集,从而有助于形成甲基卡超大型 Li 矿床。

4　结束语

Li 由于同位素分馏大和强的流体活动性,使其在地质学、地球化学研究中具有广阔的应用前景。高精度 Li 同位素测试是获取样品 Li 同位素组成的保障,也是 Li 同位素在地质应用的前提,随着 MC-ICP-MS 分析技术的不断发展,国内多家实验室已相继建立了 Li 同位素高精度分析方法,并开展了不同地质样品的 Li 同位素测试工作。研究团队所建立的 Li 同位素分析方法,分析精度达到 0.5‰,外部重现性≤±1.0‰,Li 样品用量为 100 μg/L。在此基础上,研发了流体包裹体的 Li 同位素分析方法,并建立了石英—流体 Li 同位素分馏经验公式,为利用不同类型矿床广泛发育的石英示踪成矿流体来源奠定了坚实基础。首次将 Li 同位素应用到四川呷村大型铅锌铜多金属矿床成矿流体研究中,提供了岩浆水大量参与成矿的 Li 同位素新证据,再塑了两端元流体混合过程及其空间变化,完善了呷村矿床热水成矿模型。

建立了适用于西藏本地岩石成因研究的 Li 同位素地质端元,为 Li 同位素应用于青藏高原岩石圈结构及其隆升历史研究奠定了坚实基础,研究发现印度下地壳在早—中中新世俯冲到拉萨地块之下,造成了青藏高原的隆升,而青藏高原中部在 38 Ma 仍存在洋壳残余板片,说明松潘—甘孜地体的俯冲速度较之前的估计要慢,西藏中部的隆升可能比之前认为的要晚,以前认为藏中地区早在 45~38 Ma 就开始隆升。

关键金属主要包括稀有金属、稀土金属、稀散金属和部分稀贵金属,在新能源、新材料、信息技术等新兴产业和国防建设等行业中具有不可替代的重大用途。为此,国家自然科学基金委员会于 2019 年 7 月启动了“战略性关键金属超常富集成矿动力学”重大研究计划,立足地球科学前沿和国家重大需求,重点以中低温热液矿床、花岗岩—伟晶岩型矿床、碱性岩—碳酸岩型矿床、风化—沉积型矿床为主要研究对象,以低丰度金属元素超常富集过程与驱动机制研究为主线,实现理论突破和技术创新,为发现新型资源、深度利用资源提供坚实科学基础。研究团队先后选择川西冕宁—德昌碳酸岩型稀土成矿带、四川甲基卡花岗岩—伟晶岩型 Li 矿床为研究对象,通过 Li 同位素示踪手段,对稀土和 Li 的超常富集过程进行了立典式研究,展示了 Li 同位素在花岗岩—伟晶岩型 Li 矿床和碱性岩—碳酸岩型稀土矿床研究中的良好应用前景。

致谢:感谢丁悌平研究员长期以来对本文第一作者的关心和厚爱,以此祝贺丁悌平先生八十华诞。感谢 Rudnick R. L. 院士、McDonough W. F. 教授、滕方振教授、张宏福院士、刘丛强院士、赵悦博士、苏媛娜硕士、胡文洁硕士、李真真硕士、侯可军博士、赵志琦教授、汪齐连博士、朱祥坤研究员、唐索寒研究员、田恒次副研究员、张慧娟博士、王登红研究员、李延河研究员、杨竹森研究员、杨志明研究员、宋玉财研究员、李振清副研究员、付小方教授级高工、郝雪峰高工、陈欣阳博士、孙杨博士、胡妍博士、黄天一博士、许英奎副研究员、李贤芳硕士、张玉洁硕士和向蜜硕士等在室内外给予的大力支持与帮助。感谢审稿专家提出的宝贵修改意见,谨致谢忱!

参　考　文　献　/　References

(The literature whose publishing year followed by a “&” is in Chinese with English abstract; The literature whose publishing year followed by a “#” is in Chinese without English abstract)

侯江龙, 李建康, 张玉洁, 李超. 2018. 四川甲基卡锂矿床花岗岩体 Li 同位素组成及其对稀有金属成矿的制约. 地球科学, 43(6): 2042~2054.

侯可军, 李延河, 田有荣, 秦燕, 谢桂青. 2008. MC-ICP-MS 高精度 Cu、Zn 同位素测试技术. 矿床地质, 27(6): 774~781.

侯增谦, 曲晓明, 徐明基, 付德明, 华力臣, 余金杰. 2001. 四川呷村 VHMS 矿床: 从野外观察到成矿模型. 矿床地质, 20(1): 44~56.

李贤芳, 田世洪, 王登红, 张慧娟, 张玉洁, 付小方, 郝雪峰, 侯可军, 赵悦, 秦燕, 于扬, 王海. 2020. 川西甲基卡锂矿床花岗岩与伟晶岩成因关系: U-Pb 定年、Hf—O 同位素和地球化学证据. 矿床地质, 39(2): 273~304.

李献华, 刘宇, 汤艳杰, 高钰涯, 李秋立, 唐国强. 2015. 离子探针 Li 同位素微区原位分析技术与应用. 地学前缘, 22(5): 160~170.

刘丽君, 王登红, 侯可军, 田世洪, 赵悦, 付小方, 袁蔺平, 郝雪峰. 2017. 锂同位素在四川甲基卡新三号矿脉研究中的应用. 地学前缘, 24(5): 167~171.

刘涛, 田世洪, 王登红, 张玉洁, 李贤芳, 侯可军, 杰肯·卡里木汗, 张忠利, 王永强, 赵悦, 秦燕. 2020. 新疆卡鲁安硬岩型锂矿床花岗岩与伟晶岩成因关系: 锆石 U-Pb 定年、Hf—O 同位素和全岩地球化学证据. 地质学报, 94(11): 3293~3320.

苏媛娜, 田世洪, 李真真, 侯增谦, 侯可军, 胡文洁, 高延光, 杨丹, 李延河, 杨竹森. 2011. MC-ICP-MS 高精度 Li 同位素分析方法. 地学前缘, 18(2): 304~314.

汪齐连, 赵志琦, 刘丛强, 凌宏文. 2006. 天然样品中锂的分离及其同位素比值的测定. 分析化学, 34(6): 764~768.

赵悦, 侯可军, 田世洪, 杨丹, 苏媛娜. 2015. 常用锂同位素地质标准物质的多接收器电感耦合等离子体质谱分析研究. 岩矿测试, 34(1): 28~39.

赵悦, 李延河, 胡斌, 侯可军, 范昌福, 高建飞. 2020. 碳酸盐(岩)的锂同位素组成: 一种潜在的古海水 pH 替代性指标. 地球学报, 41(5): 613~622.

Argand E. 1924. La tectonique de l'Asie. In: Proceedings of 13th International Geological Congress. 171~372.

Ballouard C, Elburg M A, Tappe S, Reinke C, Ueckermann H, Doggart S. 2020. Magmatic—hydrothermal evolution of rare metal pegmatites from the Mesoproterozoic Orange River pegmatite belt (Namaqualand, South Africa). Ore Geology Reviews, 116: 103252.

Beaumont C, Jamieson R A, Nguyen M H, Lee B. 2001. Himalayan tectonics explained by extrusion of a low-velocity channel coupled with focused surface denudation. Nature, 414: 738~742.

Bell K and Simonetti A. 2010. Source of parental melts to carbonatites——Critical isotopic constraints. Mineralogy and Petrology, 98: 77~89.

Botsyun S, Sepulchre P, Donnadieu Y, Risi C, Licht A, Rugenstein J K C. 2019. Revised paleoaltimetry data show low Tibetan Plateau elevation during the Eocene. Science, 363: 946.

Bouman C, Elliott T, Vroon P Z. 2004. Lithium inputs to subduction zones. Chemical Geology, 212: 59~79.

Candela P A, Piccoli P M. 1995. Model ore—metal partitioning from melts into vapor and vapor/brine mixtures. In Thompson J F H, Ed., Mineralogical Association of Canada, Quebec Granites, Fluids, and Ore Deposits, 23: 101~128.

Chakraborty T, Upadhyay D. 2020. The geochemical differentiation of S-type pegmatites: constraints from major—trace element and Li—B isotopic composition of muscovite and tourmaline. Contributions to Mineralogy and Petrology, 175: 60.

Chan L H, Alt J C, Teagle D A H. 2002. Lithium and lithium isotope profiles through the upper oceanic crust: a study of seawater—basalt exchange at ODP Sites 504B and 896A. Earth and Planetary Science Letters, 201: 187~201.

Chan L H, Edmond J M, Thompson G, Gillis K. 1992. Lithium isotopic composition of submarine basalts: implications for the lithium cycle in the oceans. Earth and Planetary Science Letters, 108: 151~160.

Chan L H, Kastner M. 2000. Lithium isotopic compositions of pore fluids and sediments in the Costa Rica subduction zone: implications for fluid processes and sediment contribution to the arc volcanoes. Earth and Planetary Science Letters, 183: 275~290.

Chan L H, Leeman W P, Plank T. 2006. Lithium isotopic composition of marine sediments. Geochemistry, Geophysics, Geosystems, 7: doi: 10.1029/2005GC001202.

Chan L H. 1988. Variation of lithium isotope composition in the marine environment: A preliminary report. Geochimica et Cosmochimica Acta, 52: 1711~1717.

Chen Bin, Gu Haiou, Chen Yanjiao, Sun Keke, Chen Wei. 2018. Lithium isotope behavior during partial melting of metapelites from the Jiangnan Orogen, South China: implications for the origin of REE tetrad effect of F-rich granite and associated rare-metal mineralization. Chemical Geology, 483: 372~384.

Chen Bin, Huang Chao, Zhao Hui. 2020. Lithium and Nd isotopic constraints on the origin of Li-poor pegmatite with implications for Li mineralization. Chemical Geology, 551: 119769.

Chen Jianlin, Wu Jianbin, Xu Jifeng, Dong Yanhui, Wang Baodi, Kang Zhiqiang. 2013. Geochemistry of Eocene high-Mg# adakitic rocks in the northern Qiangtang terrane, central Tibet: implications for early uplift of the plateau. Geological Society of America Bulletin, 125: 1800~1819.

Chen Jianlin, Xu Jifeng, Wang Baodi, Kang Zhiqiang, Li Jie. 2010. Origin of Cenozoic alkaline potassic volcanic rocks at KonglongXiang, Lhasa terrane, Tibetan Plateau: products of partial melting of a mafic lower-crustal source? Chemical Geology, 273: 286~299.

Chen Jianlin, Yin An, Xu Jifeng, Dong Yanhui, Kang Zhiqiang. 2017. Late Cenozoic magmatic inflflation, crustal thickening, and > 2 km of surface uplift in central Tibet. Geology, 46: 19~22.

Chen Lin, Capitanio F A, Liu Lijun, Gerya T V. 2017. Crustal rheology controls on the Tibetan plateau formation during India—Asia convergence. Nature Communications, 8: http://dx. doi. org/10.1038/ncomms15992.

Chen Yixiang, Schertl H P, Zheng Yongfei, Huang Fang, Zhou Kun, Gong Yingzeng. 2016. Mg—O isotopes trace the origin of Mg-rich fluids in the deeply subducted continental crust of Western Alps. Earth and Planetary Science Letters, 456: 157~167.

Cheng Zhiguo, Zhang Zhaochong, Aibai A, Kong Weiliang, Holtz F. 2018. The role of magmatic and post-magmatic hydrothermal processes on rare-earth element mineralization: a study of the Bachu carbonatites from the Tarim Large Igneous Province, NW China. Lithos, 314~315: 71~87.

Cheng Zhiguo, Zhang Zhaochong, Hou Tong, Santosh M, Chen Lili, Ke Shan, Xu Lijuan. 2017. Decoupling of Mg—C and Sr—Nd—O isotopes traces the role of recycled carbon in magnesiocarbonatites from the Tarim Large Igneous Province. Geochimica et Cosmochimica Acta, 202: 159~178.

Cheng Zhihui, Guo Zhengfu. 2017. Post-collisional ultrapotassic rocks and mantle xenoliths in the Sailipu volcanic field of Lhasa terrane, south Tibet: petrological and geochemical constraints on mantle source and geodynamic setting. Gondwana Research, 46: 17~42.

Chung S L, Lo C H, Lee T Y, Zhang Yuquan, Xie Yingwen, Li Xianhua, Wang Kuo-Lung, Wang Peiling. 1998. Diachronous uplift of the Tibetan plateau starting 40 Myr ago. Nature, 394: 769~773.

Copley A, Avouac J P, Wernicke B P. 2011. Evidence for mechanical coupling and strong Indian lower crust beneath southern Tibet. Nature, 472: 79~81.

Croudace I W. 1980. A possible error source in silicate wet chemistry caused by insoluble fluorides. Chemical Geology, 31: 153~155.

Deveaud S, Millot R, Villaros A. 2015. The genesis of LCT-type granitic pegmatites, as illustrated by lithium isotopes in micas. Chemical Geology, 411: 97~111.

Ding Lin, Kapp P, Yue Yahui, Lai Qingzhou. 2007. Postcollisional calc-alkaline lavas and xenoliths from the southern Qiangtang terrane, central Tibet. Earth and Planetary Science Letters, 254: 28~38.

Doroshkevich A G, Veksler I V, Klemd R, Khromova E A, Izbrodin I A. 2017. Trace-element composition of minerals and rocks in the belaya zima carbonatite complex (russia): implications for the mechanisms of magma evolution and carbonatite formation. Lithos, 284~285: 91~108.

Dupont-Nivet G, Krijgsman W, Langereis C G, Abels H A, Dai Shuang, Fang Xiaomin. 2007. Tibetan plateau aridifification linked to global cooling at the Eocene—Oligocene transition. Nature, 445: 635~638.

Fan Jingjing, Tang Gongjian, Wei Gangjian, Wang He, Xu Yigang, Wang Qiang, Zhou Jinsheng, Zhang Zhuoying, Huang Tongyu, Wang Zilong. 2020. Lithium isotope fractionation during fluid exsolution: implications for Li mineralization of the Bailongshan pegmatites in the West Kunlun, NW Tibet. Lithos, 352~353:

105236.

Flesch G D, Anderson A J, Svec H J. 1973. A secondary isotopic standard for lithium determinations. International Journal of Mass Spectrometry and Ion Processes, 12: 265~272.

Franklin J M, Gibson H L, Jonasson I R, Galley A G. 2005. Volcanogenic massive sulfide deposits. Economic Geology, 100: 523~560.

Gao Yongfeng, Wei Ruihua, Ma Peixue, Hou Zengqian, Yang Zhusen. 2009. Post-collisional ultrapotassic volcanism in the Tangra Yumco—Xuruco graben, south Tibet: constraints from geochemistry and Sr—Nd—Pb isotope. Lithos, 110: 129~139.

Goderis S, Chakrabarti R, Debaille V, Kodolányi J. 2016. Isotopes in cosmochemistry: recipe for a Solar System. Journal of Analytical Atomic Spectrometry, 31(4): 841~862.

Gourcerol B, Gloaguen E, Melleton J, Tuduri J, Galiegue X. 2019. Re-assessing the European lithium resource potential——A review of hard-rock resources and metallogeny. Ore Geology Reviews, 109: 494~519.

Guo Zhengfu, Wilson M, Liu Jiaqi, Mao Qian. 2006. Post-collisional, potassic and ultrapotassic magmatism of the northern Tibetan Plateau: constraints on characteristics of the mantle source, geodynamic setting and uplift mechanisms. Journal of Petrology, 47: 1177~1220.

Guo Zhengfu, Wilson M, Zhang Maoliang, Cheng Zhihui, Zhang Lihong. 2015. Post-collisional ultrapotassic mafic magmatism in South Tibet: products of partial melting of pyrox enite in the mantle wedge induced by roll-back and delamination of the subducted Indian continental lithosphere slab. Journal of Petrology, l56: 1365~1406.

Halama R, John T, Herms P, Hauff F, Schenk V. 2011. A stable (Li, O) and radiogenic (Sr, Nd) isotope perspective on metasomatic processes in a subducting slab. Chemical Geology, 281(3/4): 151~166.

Halama R, McDonough W F, Rudnick R L, Bell K. 2008. Tracking the lithium isotopic evolution of the mantle using carbonatites. Earth Planetary Science Letters, 265: 726~742.

Halama R, McDonough W F, Rudnick R L, Keller J, Klaudius J. 2007. The Li isotopic composition of Oldoinyo Lengai: nature of the mantle sources and lack of isotopic fractionation during carbonatite petrogenesis. Earth Planetary Science Letters, 254: 77~89.

Hall J M, Chan L H, McDonough W F, Turekian K K. 2005. Determination of the lithium isotopic composition of planktic foraminifera and its application as a paleo-seawater proxy. Marine Geology, 217: 255~265.

Hanna H D, Liu Xiaoming, Park Y R, Kay S M, Rudnick R L. 2020. Lithium isotopes may trace subducting slab signatures in Aleutian arc lavas and intrusions. Geochimica et Cosmochimica Acta, 278: 322~339.

He Maoyong, Luo Chongguang, Yang Hongjun, Kong Fancui, Li Yulong, Deng Li, Zhang Xiying, Yang Kaiyuan. 2020. Sources and a proposal for comprehensive exploitation of lithium brine deposits in the Qaidam Basin on the northern Tibetan Plateau, China: evidence from Li isotopes. Ore Geology Reviews, 117: 103277.

Hou Jianglong, Li Jiankang, Zhang Yujie, Li Chao. 2018&. Li isotopic composition and its constraints on rare metal mineralization of Jiajika two-mica granite, Sichuan Province. Earth Science, 43(6): 2042~2054.

Hou Kejun, Li Yanhe, Tian Yourong, Qin Yan, Xie Guiqing. 2008&. High precision Cu, Zn isotope measurements by multi-collector ICP-MS. Mineral Deposits, 27(6): 774~781.

Hou Zengqian, Duan Lianfeng,, Lu Yongjun, Zheng Yuanchuan, Zhu Dicheng, Yang Zhusen, Wang Baodi, Pei Yingru, Zhao Zhidan, Campbell M T. 2015a. Lithospheric architecture of the Lhasa Terrane and its control on ore deposits in the Himalayan—Tibetan Orogen. Economic Geology, 110(6): 1541~1575.

Hou Zengqian, Liu Yan, Tian Shihong, Yang Zhiming, Xie Yuling. 2015b. Formation of carbonatite-related giant REE deposits by the recycling of marine sediments. Scientific Reports, 5: 10231. DOI: 10.1038/srep10231.

Hou Zengqian, Qu Xiaoming, Xu Mingji, Fu Deming, Hua Lichen, Yu Jinjie. 2001&. The Gacun VHMS deposit in Sichuan Province: from field observation to genetic model. Mineral Deposits, 20(1): 44~56.

Hou Zengqian, Tian Shihong, Xie Yuling, Yang Zhusen, Yuan Zhongxin, Yin Shupin, Yi Longsheng, Fei Hongcai, Zou Tianren, Li Xiaoyu. 2009. The Himalayan Mianning—Dechang REE belt associated with carbonatite—alkalic complex in the eastern Indian—Asian collision zone, SW China. Ore Geology Reviews, 36: 65~89.

Hou Zengqian, Tian Shihong, Yuan Zhongxin, Xie Yuling, Yin Shupin, Yi Longsheng, Fei Hongcai, Yang Zhusen. 2006. The Himalayan collision zone carbonatites in western Sichuan, SW China: petrogenesis, mantle source and tectonic implication. Earth Planet Science Letters, 244: 234~250.

Hu Yan, Teng Fangzhen, Plank T, Huang Kangjun. 2017. Magnesium isotopic composition of subducting marine sediments. Chemical Geology, 466: 15~31.

Huang Feng, Chen Jianlin, Xu Jifeng, Wang Baodi, Li Jie, Zeng Yunchuan, Zou Jieqiong. 2015. Os—Nd—Sr isotopes in Miocene ultrapotassic rocks of southern Tibet: partial melting of a pyroxenite-bearing lithospheric mantle? Geochimica et Cosmochimica Acta, 163: 279~298.

Huang Kangjun, Teng Fangzhen, Elsenouy A, Li Wangye, Bao Zhengyu. 2013. Magnesium isotopic variations in loess: origins and implications. Earth and Planetary Science Letters, 374: 60~70.

Huang Kangjun, Teng Fangzhen, Plank T, Staudigel H, Hu Yan, Bao Zhengyu. 2018. Magnesium isotopic composition of altered oceanic crust and the global Mg cycle. Geochimica et Cosmochimica Acta, 238: 357~373.

Jeffcoate A B, Elliott T, Thomas A, Bouman C. 2004. Precise, small sample size determinations of lithium isotopic compositions of geological reference materials and modern seawater by MC-ICPMS. Geostandards and Geoanalytical Research, 28: 161~172.

Jiang Yaohui, Jiang Shaoyong, Ling Hongfei, Dai Baozhang. 2006. Low-degree melting of a metasomatized lithospheric mantle for the origin of Cenozoic Yulong monzogranite-porphyry, east Tibet: geochemical and Sr—Nd—Pb—Hf isotopic constraints. Earth and Planetary Science Letters, 241: 617~633.

Kaeter D, Barros R, Menuge J F, Chew D M. 2018. The magmatic—hydrothermal transition in rare-element pegmatites from southeast Ireland: LA-ICP-MS chemical mapping of muscovite and columbite—tantalite. Geochimica et Cosmochimica Acta, 240: 98~130.

Kisakürek B, James R H, Harris N B W. 2005. Li and δ^7Li in Himalayan rivers: proxies for silicate weathering. Earth and Planetary Science Letters, 237: 387~401.

Kosarev G, Kind R, Sobolev S V, Yuan Xiaohui, Hanka W, Oreshin S. 1999. Seismic evidence for a detached Indian lithosphere mantle beneath Tibet. Science, 283: 1306~1309.

Krienitz M S, Garbe-Schönberg C D, Romer R L, Meixner A, Haase K M, Stroncik N A. 2012. Lithium isotope variations in ocean island basalts——Implications for the development of mantle heterogeneity. Journal of Petrology, 53: 2333~2347.

Lai Shaocong, Qin Jiangfeng. 2013. Adakitic rocks derived from the partial melting of subducted continental crust: evidence from the Eocene volcanic rocks in the northern Qiangtang block. Gondwana Research, 23: 812~824.

Le Bas M J. 1989. Diversification of carbonatite. In: Bell K. (ed.). Carbonatites: Genesis and Evolution. London: Unwin Hyman. 428~447.

Li Jiankang, Chou I-Ming. 2016. An occurrence of metastable cristobalite in spodumene-hosted crystal-rich inclusions from Jiajika pegmatite deposit, China. Journal of Geochemical Exploration, 171: 29~36.

Li Jiankang, Chou I-Ming. 2017. Homogenization experiments of crystal-rich inclusions in spodumene from Jiajika lithium deposit, China, under elevated external pressures in a hydrothermal diamond-anvil Cell. Geofluids, 2017: 1~12.

Li Jiankang, Zou Tianren, Liu Xifang, Wang Denghong, Ding Xin. 2015. The metallogenetic regularities of lithium deposits in China. Acta Geologica Sinica, 89: 652~670.

Li Jie, Huang Xiaolong, Wei Gangjian, Liu Ying, Ma Jinlong, Han Li, He Pengli. 2018. Lithium isotope fractionation during magmatic differentiation and hydrothermal processes in rare-metal granites. Geochimica et Cosmochimica Acta, 240: 64~79.

Li Wangye, Teng Fangzhen, Ke Shan, Rudnick R L, Gao Shan, Wu Fuyuan, Chappell B W. 2010. Heterogeneous magnesium isotopic composition of the upper continental crust. Geochimica et Cosmochimica Acta, 74: 6867~6884.

Li Wenshuai, Liu Xiaoming, Chadwick O A. 2020. Lithium isotope behavior in Hawaiian regoliths: soil—atmosphere—biosphere exchanges. Geochimica et Cosmochimica Acta, 285: 175~192.

Li Xianfang, Tian Shihong, Wang Denghong, Zhang Huijuan, Zhang Yujie, Fu Xiaofang, Hao Xuefeng, Hou Kejun, Zhao Yue, Qin Yan, Yu Yang, Wang Hai. 2020&. Genetic relationship between pegmatite and granite in Jiajika lithium deposit in western Sichuan: evidence from zircon U-Pb dating, Hf—O isotope and geochemistry. Mineral Deposits, 39(2): 273~304.

Li Xianhua, Liu Yu, Tang Yanjie, Gao Yuya, Li Qiuli, Tang Guoqiang. 2015&. In situ Li isotopic microanalysis using SIMS and its applications. Earth Science Frontiers, 22(5): 160~170.

Liu Dong, Zhao Zhidan, DePaolo D J, Zhu Dicheng, Meng Fanyi, Shi Qingshang, Wang Qing. 2017. Potassic volcanic rocks and adakitic intrusions in southern Tibet: insights into mantle—crust interaction and mass transfer from Indian plate. Lithos, 268~271: 48~64.

Liu Dong, Zhao Zhidan, Zhu Dicheng, Niu Yaoling, DePaolo D J, Harrison T M, Mo Xuanxue, Dong Guochen, Zhou Su, Sun Chenguang, Zhang Zhaochong, Liu Junlai. 2014. Postcollisional potassic and ultrapotassic rocks in southern Tibet: mantle and crustal origins in response to India—Asia collision and convergence. Geochimica et Cosmochimica Acta, 143: 207~231.

Liu Dong, Zhao Zhidan, Zhu Dicheng, Niu Yaoling, Widom E, Teng Fangzhen, DePaolo D J, Ke Shan, Xu Jifeng, Wang Qing, Mo Xuanxue. 2015. Identifying mantle carbonatite metasomatism through Os—Sr—Mg isotopes in Tibetan ultrapotassic rocks. Earth and Planetary Science Letters, 430: 458~469.

Liu Haiyang, Sun He, Xiao Yilin, Wang Yangyang, Zeng Lingsen, Li Wangye, Guo Haihao, Yu Huimin, Pack Andreas. 2019. Lithium isotope systematics of the Sumdo Eclogite, Tibet: tracing fluid/rock interaction of subducted low-T altered oceanic crust. Geochimica et Cosmochimica Acta, 246: 385~405.

Liu Jiayi, Liu Quanyou, Meng Qingqiang, Zhu Dongya, Liang Xinping. 2020. The distribution of lithium in nature and the application of lithium isotope tracing. IOP Conference Series: Earth and Environmental Science, 600: 012018.

Liu Lijun, Wang Denghong, Hou Kejun, Tian Shihong, Zhao Yue, Fu Xiaofang, Yuan Linping, Hao Xuefeng. 2017&. Application of lithium isotope to Jiajika new No. 3 pegmatite lithium polymetallic vein in Sichuan. Earth Science Frontiers, 24(5): 167~171.

Liu Tao, Tian Shihong, Wang Denghong, Zhang Yujie, Li Xianfang, Hou Kejun, Jieken·Kalimuhan, Zhang Zhongli, Wang Yongqiang, Zhao Yue, Qin Yan. 2020&. Genetic relationship between granite and pegmatite in Kalu'an hard-rock-type lithium deposit in Xinjiang: results from zircon U-Pb dating, Hf—O isotopes and whole-rock geochemistry. Acta Geologica Sinica, 94(11): 3293~3320.

Liu Pingping, Teng Fangzhen, Dick H J B, Zhou Meifu, Chung S L. 2017. Magnesium isotopic composition of the oceanic mantle and oceanic Mg cycling. Geochimica et Cosmochimica Acta, 206: 151~165.

Liu Yan and Hou Zengqian. 2017. A synthesis of mineralization styles with an integrated genetic model of carbonatite—syenite-hosted REE deposits in the Cenozoic Mianning—Dechang REE metallogenic belt, the eastern Tibetan Plateau, southwestern China. Journal of Asian Earth Sciences, 137: 35~79.

London D. 2018. Ore-forming processes within granitic pegmatites. Ore Geology Reviews, 101: 349~383.

Lü Zhenghang, Zhang Hui, Tang Yong, Liu Yunlong, Zhang Xin. 2018. Petrogenesis of syn-orogenic rare metal pegmatites in the Chinese Altai: evidences from geology, mineralogy, zircon U-Pb age and Hf isotope. Ore Geology Reviews, 95: 161~181.

Maffre P, Goddéris Y, Vigier N, Moquet J S, Carretier S. 2020. Modelling the riverine δ^7Li variability throughout the Amazon Basin. Chemical Geology, 532: 119336.

Magna T, Ionov D A, Oberli F, Wiechert U H. 2008. Links between mantle metasomatism and lithium isotopes: evidence from glass-bearing and cryptically metasomatized xenoliths from Mongolia. Earth and Planetary Science Letters, 276: 214~222.

Magna T, Wiechert U H, Halliday A N. 2004. Low-blank isotope ratio measurement of small samples of lithium using multiple-collector ICPMS. International Journal of Mass Spectrometry and Ion Processes, 239: 67~76.

Marschall H R, Altherr R, Gméling K, Kasztovszky Z. 2009. Lithium, boron and chlorine as tracers for metasomatism in high-pressure metamorphic rocks: A case study from Syros (Greece). Mineralogy and Petrology, 95: 291~302.

Marschall H R, Pogge von Strandmann P A E, Seitz H M, Elliott T, Niu Yaoling. 2007. The lithium isotopic composition of orogenic eclogites and deep subducted slabs. Earth and Planetary Science Letters, 262: 563~580.

Martins T, Roda-Robles E, Lima A, De Parseval P. 2012. Geochemistry and evolution of micas in the Barroso—Alvãopegmatite field, northern Portugal. Canadian Mineralogist, 50: 1117~1119.

Michils E, Bivre P D. 1983. Absolute isotopic composition and the atomic weight of a natural sample of lithium. International Journal of Mass Spectrometry and Ion Processes, 49: 264~274.

Miller C, Schuster R, Klotzli U, Frank W, Grasemann B. 1999. Post-collisional potassic and ultrapotassic magmatism in SW Tibet: geochemical and Sr—Nd—Pb—O isotopic constraints for mantle

source characteristics and petrogenesis. Journal of Petrology, 83: 5361~5375.

Molnar P, Tapponnier P. 1975. Cenozoic tectonics of Asia: effects of a continental collision. Science, 189: 419~426.

Moriguti T, Nakamura E. 1998. High-yield lithium separation and the precise isotopic analysis for natural rock and aqueous samples. Chemical Geology, 145: 91~104.

Mulja T, Williams-Jones A E. 2018. The physical and chemical evolution of fluids in rare-element granitic pegmatites associated with the Lacorne pluton, Québec, Canada. Chemical Geology, 493: 281~297.

Müller A, Romer R L, Pedersen R B. 2017. The sveconorwegian pegmatite province thousands of pegmatites without parental granites. Canadian Mineralogist, 55: 283~315.

Murphy M J, Porcelli D, von Strandmann P A E P, Hirst C A, Kutscher L, Katchinoff J K, Mörth C M, Maximov T, Andersson P S. 2019. Tracing silicate weathering processes in the permafrost-dominated Lena River watershed using lithium isotopes. Geochimica et Cosmochimica Acta, 245: 154~171.

Nábělek J, György H, Vergne J, Sapkota S, Kafle B, Jiang Mei, Su Heping, Chen John, Huang Bor-Shouh, Hi-CLIMB Team. 2009. Underplating in the Himalaya—Tibet collision zone revealed by the Hi-CLIMB experiment. Science, 325: 1371~1374.

Nadeau O, Mick E, Robidoux P, Grassa F, Brusca L, Voinot A, Leybourne M I. 2020. Lithium isotopes and Cu—Au concentrations in hydrothermal alterations from Solfatara Volcano, Campi Flegrei caldera complex, and La Fossa volcano, Vulcano Island, Italy: insights into epithermal ore forming environments. Ore Geology Reviews, 130: 103934.

Ottolini L, Laporte D, Raffone N, Devidal J L, Molière O P G C. 2009. New experimental determination of Li and B partition coefficients during upper mantle partial melting. Contributions to Mineralogy and Petrology, 157: 313~325.

Ou Quan, Wang Qiang, Wyman D A, Zhang Haixiang, Yang Jinhui, Zeng Jipeng, Hao Lulu, Chen Yiwei, Liang He, Qi Yue. 2017. Eocene adakitic porphyries in the central—northern Qiangtang Block, central Tibet: partial melting of thickened lower crust and implications for initial surface uplifting of the plateau. Journal of Geophysical Research: Solid Earth, 122: 1025~1053.

Owens T J and Zandt G. 1997. Implications of crustal property variations for models of Tibetan plateau evolution. Nature, 387: 37~43.

Pati J K, Reimold W U, Hauser N. 2018. Comment on "Anatomy of impactites and shocked zircon grains from Dhala reveals Paleoproterozoic meteorite impact in the Archean basement rocks of Central India" by Li et al. Gondwana Research, 54: 81~101.

Penniston-Dorland S C, Liu X M, Rudnick R L. 2017. Lithium Isotope Geochemistry. In: Teng F Z, Watkins J M, Dauphas N (Eds.) Non-traditional stable isotopes. Reviews in Mineralogy & Geochemistry, 82: 165~217.

Qi Huihui, Ma Chuanming, He Zekang, Hu Xiaojing, Gao Lin. 2019. Lithium and its isotopes as tracers of groundwater salinization: A study in the southern coastal plain of Laizhou Bay, China. Science of the Total Environment, 650: 878~890.

Qiu L, Rudnick R L, McDonough W F, Merriman R J. 2009. Li and ^{7}Li in mudrocks from the British Caledonides: metamorphism and source influences. Geochimica et Cosmochimica Acta, 73: 7325~7340.

Richter F M, Davis A M, DePaolo D J, Watson E B. 2003. Isotope fractionation by chemical diffusion between molten basalt and rhyolite. Geochimica et Cosmochimica Acta, 67: 3905~3923.

Roda-Robles E, Villaseca C, Pesquera A, Gil-Crespo P P, Vieira R, Lima A, Garate-Olave I. 2018. Petrogenetic relationships between Variscan granitoids and Li—(F—P)-rich aplite—pegmatites in the Central Iberian Zone: geological and geochemical constraints and implications for other regions from the European Variscides. Ore Geology Reviews, 95: 408~430.

Rosner M, Ball L, Peucker-Ehrenbrink B, Blusztajn J, Bach W, Erzinger J. 2007. A simplified, accurate and fast method for lithium isotope analysis of rocks and fluids, and δ^{7}Li values of seawater and rock reference materials. Geostandards and Geoanalytical Research, 31: 77~88.

Rowley D B, Currie B S. 2006. Palaeo-altimetry of the late Eocene to Miocene Lunpola basin, central Tibet. Nature, 439: 677~681.

Rudnick R L, Tomasack P B, Njo H B, Gardner L R. 2004. Extreme lithium isotopic fractionation during continental weathering revealed in saprolites from South Carolina. Chemical Geology, 212: 45~57.

Ryan J G, Langmuir C H. 1987. The systematics of lithium abundances in young volcanic rocks. Geochimica et Cosmochimica Acta, 51: 1727~1741.

Saenger C, Wang Zhengrong. 2014. Magnesium isotope fractionation in biogenic and abiogenic carbonates: implications for paleoenvironmental proxies. Quaternary Science Reviews, 90: 1~21.

Sauzéat L, Rudnick R L, Chauvel C, Garçon M, Tang Ming. 2015. New perspectives on the Li isotopic composition of the upper continental crust and its weathering signature. Earth and Planetary Science Letters, 428: 181~192.

Searle M P, Elliott J R, Phillips R J, Chung S L. 2011. Crustal—lithospheric structure and continental extrusion of Tibet. Journal of the Geological Society, 168: 633~672.

Seitz H M, Woodland A B. 2000. The distribution of lithium in peridotitic and pyroxenitic mantle lithologies: An indicator of magmatic and metasomatic processes. Chemical Geology, 166: 47~64.

Seyedali M, Coogan L A, Gillis K M. 2021. Li isotope exchange during low-temperature alteration of the upper oceanic crust at DSDP Sites 417 and 418. Geochimica et Cosmochimica Acta, 294: 160~173.

Shen Xingyan,, Wan Shiming, France-Lanord C, Clift P D, Tada R, Révillon S, Shi Xuefa, Zhao Debo, Li Yangguang, Yin Xuebo, Song Zehua, Li Anchun. 2017. History of Asian eolian input to the Sea of Japan since 15 Ma: links to Tibetan uplift or global cooling? Earth and Planetary Science Letters, 474: 296~308.

Shi Danian, Wu Zhenhan, Klemperer S L, Zhao Wenjing, Xue Guangqi, Su Heping. 2015. Receiver function imaging of crustal suture, steep subduction, and mantle wedge in the eastern India—Tibet continental collision zone. Earth and Planetary Science Letters, 414: 6~15.

Simmons W B, Webber K L. 2008. Pegmatite genesis: state of the art. European Journal of Mineralogy, 20: 421~438.

Simons K K, Harlow G E, Brueckner H K, Goldstein S L, Sorensen S S, Hemming N G, Langmuir C H. 2010. Lithium isotopes in Guatemalan and Franciscan HP—LT rocks: insights into the role of sediment-derived fluids during subduction. Geochimica et Cosmochimica Acta, 74: 3621~3641.

Su Aina, Tian Shihong, Li Zhenzhen, Hou Zengqian, Hou Kejun, Hu Wenjie, Gao Yanguang, Yang Dan, Li Yanhe, Yang Zhusen. 2011&. High-precision measurement of lithium isotopes using MC-ICP-MS. Earth Science Frontiers, 18(2): 304~314.

Su Benxun, Gu Xiaoyan, Deloule E, Zhang Hongfu, Li Qiuli, Li Xianhua, Vigier N, Tang Yanjie, Tang Guoqiang, Liu Yu, Pang

K, Brewer A, Mao Qian, Ma Yuguang. 2015. Potential orthopyroxene, clinopyroxene and olivine reference materials for in situ lithium isotope determination. Geostandards and Geoanalytical Research, 39: 357~369.

Su Benxun, Zhang Hongfu, Deloule E, Sakyi P A, Xiao Yan, Tang Yanjie, Hu Yan, Ying Jifeng, Liu Pingping. 2012. Extremely high Li and low δ^7Li signatures in the lithospheric mantle. Chemical Geology, 292~293: 149~157.

Su Jianhui, Zhao Xinfu, Li Xiaochun, Hu Wei, Chen Mi, Xiong Yilin. 2019. Geological and geochemical characteristics of the Miaoya syenite—carbonatite complex, Central China: implications for the origin of REE—Nbenriched carbonatite. Ore Geology Reviews, 113: 103101.

Sun Jimin, Xu Qinghai, Liu Weiming, Zhang Zhenqing, Xue Lei, Zhao Ping. 2014. Palynological evidence for the latest Oligocene—early Miocene paleoelevation estimate in the Lunpola Basin, central Tibet. Palaeogeography, Palaeoclimatology, Palaeoecology, 399: 21~30.

Tan Dongbo, Xiao Yilin, Sun He, Li Wangye, Dai Liqun, Liu Haiyang, Tong Fengtai. 2020. Lithium isotopic compositions of post-collisional mafic—ultramafic rocks from Dabieshan, China: implications for recycling of deeply subducted continental crust. Lithos, 352~353: 105327.

Tapponnier P, Xu Zhiqin, Roger F, Meyer B, Arnaud N, Wittlinger G, Yang Jingsui. 2001. Geology——Oblique stepwise rise and growth of the Tibet plateau. Science, 294: 1671~1677.

Teng Fangzhen, Dauphas N, Watkins J M. 2017. Non-traditional stable isotopes: retrospective and prospective. Reviews in Mineralogy and Geochemistry, 82: 165~217.

Teng Fangzhen, Hu Yan, Chauvel C. 2016. Magnesium isotope geochemistry in arc volcanism. Proceedings of the National Academy of Sciences of the United States of America, 113: 7082~7087.

Teng Fangzhen, McDonough W F, Rudnick R L, Dalpé C, Tomascak P B, Chappell B W. 2004. Lithium isotopic composition and concentration of the upper continental crust. Geochimica et Cosmochimica Acta, 68: 4167~4178.

Teng Fangzhen, McDonough W F, Rudnick R L, Walker R J, Sirbescu M L. 2006a. Lithium isotopic systematics of granites and pegmatites from the Black Hills, South Dakota. American Mineralogist, 91: 1488~1498.

Teng Fangzhen, McDonough W F, Rudnick R L, Walker R J. 2006b. Diffusion-driven extreme lithium isotopic fractionation in country rocks of the Tin Mountain pegmatite. Earth Planetary Science Letters, 243: 701~710.

Teng Fangzhen, McDonough W F, Rudnick R L, Wing B A. 2007. Limited lithium isotopic fractionation during progressive metamorphic dehydration in metapelites: a case study from the Onawa contact aureole, Maine. Chemical Geolog, 239: 1~12.

Teng Fangzhen, Rudnick R L, McDonough W F, Gao Shan, Tomascak P B, Liu Yongsheng. 2008. Lithium isotopic composition and concentration of the deep continental crust. Chemical Geology, 255: 47~59.

Teng Fangzhen, Rudnick R L, McDonough W F, Wu Fuyuan. 2009. Lithium isotopic systematics of A-type granites and their mafic enclaves: further constraints on the Li isotopic composition of the continental crust. Chemical Geology, 262: 370~379.

Teng Fangzhen, Yang Wei, Rudnick R L, Hu Yan. 2013. Heterogeneous magnesium isotopic composition of the lower continental crust: a xenolith perspective. Geochemistry, Geophysics, Geosystems, 14: 3844~3856.

Thomas R, Davidson P, Badanina E. 2009. A melt and fluid inclusion assemblage in beryl from pegmatite in the Orlovka amazonite granite, East Transbaikalia, Russia: implications for pegmatite-forming melt systems. Mineralogy and Petrology, 96: 129~140.

Thomas R, Davidson P. 2012. Water in granite and pegmatite-forming melts. Ore Geology Reviews, 46: 32~46.

Tian Hengci, Teng Fangzhen, Hou Zengqian, Tian Shihong, Yang Wei, Chen Xinyang, Song Yucai. 2020. Magnesium and lithium isotopic evidence for a remnant oceanic slab beneath Central Tibet. Journal of Geophysical Research: Solid Earth, 125: e2019JB018197.

Tian Shihong, Hou Zengqian, Chen Xinyang, Tian Hengci, Gong Yingli, Yang Zhusen, Huang Tianyi, Li Xianfang, Mo Xuanxue. 2020b. Magnesium isotopic behaviors between metamorphic rocks and their associated leucogranites, and implications for Himalayan orogenesis. Gondwana Research, 87: 23~40.

Tian Shihong, Hou Zengqian, Mo Xuanxue, Tian Yuheng, Zhao Yue, Hou Kejun, Yang Zhusen, Hu Wenjie, Li Xianfang, Zhang Yujie. 2020a. Lithium isotopic evidence for subduction of the Indian lower crust beneath southern Tibet. Gondwana Research, 77: 168~183.

Tian Shihong, Hou Zengqian, Su Aina, HouKejun, Hu Wenjie, Li Zhenzhen, Zhao Yue, Gao Yangguang, Li Yanhe, Yang Dan, Yang Zhusen. 2012. Separation and precise measurement of lithium isotopes in there reference materials using multi collector—inductively coupled plasma mass spectrometry. Acta Geologica Sinica, 86(5): 1297~1305.

Tian Shihong, Hou Zengqian, Su Aina, Qiu Lin, Mo Xuanxue, Hou Kejun, Zhao Yue, Hu Wenjie, Yang Zhusen. 2015. The anomalous lithium isotopic signature of Himalayan collisional zone carbonatites in western Sichuan, SW China: enriched mantle source and petrogenesis. Geochimica et Cosmochimica Acta, 159: 42~60.

Tian Shihong, Hou Zengqian, Tian Yuheng, Zhao Yue, Hou Kejun, Li Xianfang, Zhang Yujie, Hu Wenjie, Mo Xuanxue, Yang Zhusen, Li Zhenqing, Zhao Miao. 2018. Lithium content and isotopic composition of the juvenile lower crust in southern Tibet. Gondwana Research, 62: 198~211.

Tian Shihong, Yang Zhusen, Hou Zengqian, Mo Xuanxue, Hu Wenjie, Zhao Yue, Zhao Xiaoyan. 2017a. Subduction of the Indian lower crust beneath southern Tibet revealed by the post-collisional potassic and ultrapotassic rocks in SW Tibet. Gondwana Research, 41: 29~50.

Tian Shihong, Zhao Yue, Hou Zengqian, Tian Yuheng, Hou Kejun, Li Xianfang, Yang Zhusen, Hu Wenjie, Mo Xuanxue, Zheng Yuanchuan. 2017b. Lithium isotopic composition and concentration of Himalayan leucogranites and the Indian lower continental crust. Lithos, 284~285: 416~428.

Tilmann F, Ni Jamse, INDEPTH III Seismic Team. 2003. Seismic imaging of the downwelling Indian lithosphere beneath central Tibet. Science, 300: 1424 ~1427.

Tilton G R, Bryce J G, Mateen A. 1998. Pb—Sr—Nd isotope data from 30 and 300 Ma collision zone carbonatites in Northwest Pakistan. Journal of Petrology, 39: 1865 ~1874.

Tomascak P B, Magna T S, Dohmen R. 2016. Advances in lithium isotope geochemistry. Switzerland: Springer International Publishing. 1 ~195.

Tomascak P B, Carlson R W, Shirey S B. 1999b. Accurate and precise determination of Li isotopic compositions by multi-collector sector ICP-MS. Chemical Geology, 158: 145~154.

Tomascak P B, Langmuir C H. 1999. Lithium isotope variability in MORB. EOS, 80: F1086~1087.

Tomascak P B, Tera F, Helz R T, Walker R J. 1999a. The absence of

lithium isotope fractionation during basalt differentiation: new measurements by multicollector sector ICP-MS. Geochimica et Cosmochimica Acta, 63: 907~910.

Tommasini S, Avanzinelli R, Conticelli S. 2011. The Th/La and Sm/La conundrum of the Tethyan realm lamproites. Earth Planet Science Letters, 301: 469~478.

Wang Qiang, Wyman D A, Xu Jifeng, Dong Yanhui, Vasconcelos P M, Pearson N, Wan Yusheng, Dong Han, Li Chaofeng, Yu Yuanshan, Zhu Tongxing, Feng Xintao, Zhang Qiyue, Zi Feng, Chu Zhuyin. 2008. Eocene melting of subducting continental crust and early uplifting of central Tibet: evidence from central—western Qiangtang high-K calc-alkaline andesites, dacites and rhyolites. Earth and Planetary Science Letters, 272: 158~171.

Wang Qilian, Zhao Zhiqi, Liu Congqiang, Ling Hongwen. 2006&. Separation and isotopic determination of lithium in Natural Samples. Analytical Chemistry, 34(6): 764~768.

Willett S D, Beaumont C. 1994. Subduction of Asian lithospheric mantle beneath Tibet inferred from models of continental collision. Nature, 369: 642 ~645.

Wunder B, Meixner A, Romer R L, Heinrich W. 2006. Temperature-dependent isotopic fractionation of lithium between clinopyroxene and high-pressure hydrous fluids. Contributions to Mineralogy and Petrology, 151: 112 ~120.

Xiao Yan, Zhang Hongfu, Deloule E, Su Benxun, Tang Yanjie, Sakyi P A, Hu Yan, Ying Jifeng. 2015. Large lithium isotopic variations in minerals from peridotite xenoliths from the Eastern North China Craton. The Journal of Geology, 123: 79 ~94.

Xiao Yan, Zhang Hongfu, Su Benxun, Zhu Bin, Chen Beibei, Chen Chen, Sakyi P A. 2017. Partial melting control of lithium concentrations and isotopes in the Cenozoic lithospheric mantle beneath Jiande area, the Cathaysia block of SE China. Chemical Geology, 466: 750 ~761.

Xie Yuling, Hou Zengqian, Goldfarb R, Guo Xiang, Wang Lei. 2016. Rare earth element deposits in China. Reviews in Economic Geology, 18: 115~136.

Xie Yuling, Verplanck P L, Hou Zengqian, Zhong Richen. 2019. Rare earth element deposits in China: a review and new understandings. SEG Special Publications, 22: 509~552.

Xu Qiang, Zhao Junmeng, Yuan Xiaohui, Liu Hongbing, Pei Shunping. 2015. Mapping crustal structure beneath southern Tibet: seismic evidence for continental crustal underthrusting. Gondwana Research, 27: 1487~1493.

Xu Zhiqin, Fu Xiaofang, Wang Rucheng, Li Guangwei, Zheng Yilong, Zhao Zhongbao, Lian Dongyan. 2020. Generation of lithium-bearing pegmatite deposits within the Songpan—Garze orogenic belt, East Tibet. Lithos, 354~355: 105281.

Yang Dan, Hou Zengqian, Zhao Yue, Hou Kejun, Yang Zhiming, Tian Shihong, Fu Qiang. 2015. Lithium isotope traces magmatic fluid in a seafloor hydrothermal system. Scientific Reports, 5: 13812. DOI: 10.1038/srep13812.

Yang Kaihui, Scott S D. 2002. Magmatic degassing of volatiles and ore metals into a hydrothermal system on the modern sea floor of the eastern Manus back-arc basin, western Pacific. Economic Geology, 97: 1079~1100.

Yang Kuifeng, Fan Hongrui, Pirajno F, Li Xiaochun. 2019. The Bayan Obo (China) giant REE accumulation conundrum elucidated by intense magmatic differentiation of carbonatite. Geology, 47: 1198~1202.

Yang Wei, Teng Fangzhen, Li Wangye, Liu Sheng'ao, Ke Shan, Liu Yongsheng, Zhang Hongfu, Gao Shan. 2016. Magnesium isotopic composition of the deep continental crust. American Mineralogist, 101: 243~252.

You C F, Castillo P R, Gieskes J M. 1996. Trace element behavior in hydrothermal experiments: implications for fluid processes at shallow depths in subduction zones. Earth Planet Science Letters, 140: 41~52.

You C F, Chan L H. 1996. Precise determination of lithium isotopic composition in low concentration natural samples. Geochimica et Cosmochimica Acta, 60: 909~915.

Zhang Hongfu, Deloule E, Tang Yanjie, Ying Jifeng. 2010. Melt/rock interaction in remains of refertilized Archean lithosphericmantle in Jiaodong Peninsula, North China Craton: Li isotopic evidence. Contributions to Mineralogy and Petrology, 160: 261~277.

Zhang Huijuan, Tian Shihong, Wang Denghong, Li Xianfang, Liu Tao, Zhang Yujie, Fu Xiaofang, Hao Xuefeng, Hou Kejun, Zhao Yue, Yan Qin. 2021. Lithium isotope behavior during magmatic differentiation and fluid exsolution in the Jiajika granite—pegmatite deposit, Sichuan, China. Ore Geology Reviews, https://doi.org/10.1016/j.oregeorev.2021.104139.

Zhang Lihong, Guo Zhengfu, Zhang Maoliang, Cheng Zhihui, Sun Yutao. 2017. Post-collisional potassic magmatism in the eastern Lhasa terrane, South Tibet: products of partial melting of mélanges in a continental subduction channel. Gondwana Research, 41: 9~28.

Zhao Yue, Li Yanhe, Hu Bin, Hou Kejun, Fan Changfu, Gao Jianfei. 2020&. Lithium isotopic composition of marine carbonate rocks: A new proxy for Paleo-pH reconstruction. Acta Geoscientica Sinica, 41(5): 613~622.

Zhao Yue, Hou Kejun, Tian Shihong, Yang Dan, Su Aina. 2015&. Study on measurements of lithium isotopic compositions for common standard reference materials using MC-ICP-MS. Rock and Mineral Analysis, 34(3): 28~39.

Zhao Zhidan, Mo Xuanxue, Dilek Y, Niu Yaoling, Depaolo D J, Robinson P, Zhu Dicheng, Sun Chenguang, Dong Guochen, Zhou Su, Luo Zhaohua, Hou Zengqian. 2009. Geochemical and Sr—Nd—Pb—O isotopic compositions of the post-collisional ultrapotassic magmatism in SW Tibet: petrogenesis and implications for India intra-continental subduction beneath southern Tibet. Lithos, 113: 190~212.

Zhu Dicheng, Mo Xuanxue, Niu Yaoling, Zhao Zhidan, Wang Liquan, Liu Yongsheng, Wu Fuyuan. 2009. Geochemical investigation of early Cretaceous igneous rocks along an east—west traverse throughout the central Lhasa Terrane, Tibet. Chemical Geology, 268: 298~312.

Zhu Dicheng, Zhao Zhidan, Niu Yaoling, Dilek Y, Hou Zengqian, Mo Xuanxue. 2013. Origin and pre-Cenozoic evolution of the Tibetan Plateau. Gondwana Research, 23: 1429~1454.

Zhu Dicheng, Zhao Zhidan, Niu Yaoling, Mo Xuanxue, Chung Sunlin, Hou Zengqian, Wang Liquan, Wu Fuyuan. 2011. The Lhasa Terrane: record of a microcontinent and its histories of drift and growth. Earth and Planetary Science Letters, 301: 241~255.

Lithium isotopic solution analysis using MC-ICP-MS and its applications

TIAN Shihong[1, 2], LU Na[1], HOU Zengqian[3], SU Benxun[4, 5], XIAO Yan[6], YANG Dan[2]

1) *State Key Laboratory of Nuclear Resources and Environment*, *East China University of Technology*, *Nanchang*, 330013;

2) *MNR Key Laboratory of Metallogeny and Mineral Assessment*, *Institute of Mineral Resources*, *Chinese Academy of Geological Sciences*, *Beijing*, 100037;

3) *Institute of Geology*, *Chinese Academy of Geological Sciences*, *Beijing*, 100037;

4) *Key Laboratory of Mineral Resources*, *Institute of Geology and Geophysics*, *Chinese Academy of Sciences*, *Beijing*, 100029;

5) *University of Chinese Academy of Sciences*, *Beijing*, 100049;

6) *State Key Laboratory of Lithospheric Evolution*, *Institute of Geology and Geophysics*, *Chinese Academy of Sciences*, *Beijing*, 100029

Objectives: Lithium isotopes are one of the newly developed non-traditional stable isotope tracers. This isotopic system has been gaining increasing interest in fingerprinting geologic and geochemical processes. At present, lithium isotopic solution analyses mainly include thermal ionization mass spectrometry (TIMS) and multi-collector inductively coupled plasma mass spectrometry (MC-ICP-MS). Compared with TIMS, MC-ICP-MS has many advantages, such as higher analysis accuracy and precision, less sample consumption, faster analysis speed and so on.

Methods: In recent years, the research team have established high-precision measurement of lithium isotopes by MC-ICP-MS, which has achieved good results in the determination of lithium isotopes in natural samples, reference materials and quartz inclusions.

Results: Based on these analytical methods, we have established the Li isotopic geological endmembers, which are applicable to the study of the origin of local rocks in Tibet. In addition, we have applied Li isotopes to the lithospheric structure and uplift history of the Qinghai—Tibet Plateau, the enrichment mechanism of carbonatite-type rare earth deposits in western Sichuan, the source of ore-forming fluids of Gacun volcanogenic massive sulfide (VMS) deposits in Sichuan and the enrichment mechanism of Jiajika hard-rock lithium deposits in Sichuan.

Conclusions: In this paper, we present these representative applications in detail in order to deepen the understanding of lithium isotopic solution analysis and show its good application prospects in geochemical research.

Keywords: Li isotopes; MC-ICP-MS; geological endmembers; geological applications

Acknowledgements: This research was financially supported by grants from the Natural Science Foundation of China (No. 41773014), the Jiangxi Province and the East China University of Technology (No. 1410000874). The first writer would like to express his gratitude to Professor DING Tiping for his long-term care and kindness to the first author of this article. Congratulations to Professor DING Tiping on his 80th birthday. We would like to express our heartfelt thanks to all reviewers and editors for their valuable suggestions, and to the all of the teachers and project team members for their help in the field work and laboratory testing.

First author: TIAN Shihong, male, born in 1973, professor, mainly engaged in isotope geochemistry and ore deposit; Email: s. h. tian@163. com

Manuscript received on: 2021-04-03; Accepted on: 2021-06-04; Network published on: 2021-06-20

Doi: 10. 16509/j. georeview. 2021. 06. 081 **Edited by**: LIU Zhiqiang